Available online at www.sciencedirect.com

ScienceDirect

Geochimica et Cosmochimica Acta 75 (2011) 4351–4376

Geochimica et Cosmochimica Acta

www.elsevier.com/locate/gca

A thermodynamic model for the prediction of phase equilibria and speciation in the H_2O–CO_2–NaCl–$CaCO_3$–$CaSO_4$ system from 0 to 250 °C, 1 to 1000 bar with NaCl concentrations up to halite saturation

Jun Li, Zhenhao Duan *

Key Laboratory of the Earth's Deep Interior, Institute of Geology and Geophysics, Chinese Academy of Sciences, Beijing 100029, China

Received 15 November 2010; accepted in revised form 12 May 2011; available online 20 May 2011

Abstract

A thermodynamic model is developed for the calculation of both phase and speciation equilibrium in the H_2O–CO_2–NaCl–$CaCO_3$–$CaSO_4$ system from 0 to 250 °C, and from 1 to 1000 bar with NaCl concentrations up to the saturation of halite. The vapor–liquid–solid (calcite, gypsum, anhydrite and halite) equilibrium together with the chemical equilibrium of H^+, Na^+, Ca^{2+}, $CaHCO_3^+, Ca(OH)^+, OH^-, Cl^-$, $HCO_3^-, HSO_4^-, SO_4^{2-}$, $CO_3^{2-}, CO_{2(aq)}, CaCO_{3(aq)}$ and $CaSO_{4(aq)}$ in the aqueous liquid phase as a function of temperature, pressure and salt concentrations can be calculated with accuracy close to the experimental results.

Based on this model validated from experimental data, it can be seen that temperature, pressure and salinity all have significant effects on pH, alkalinity and speciations of aqueous solutions and on the solubility of calcite, halite, anhydrite and gypsum. The solubility of anhydrite and gypsum will decrease as temperature increases (e.g. the solubility will decrease by 90% from 360 K to 460 K). The increase of pressure may increase the solubility of sulphate minerals (e.g. gypsum solubility increases by about 20–40% from vapor pressure to 600 bar). Addition of NaCl to the solution may increase mineral solubility up to about 3 molality of NaCl, adding more NaCl beyond that may slightly decrease its solubility. Dissolved CO_2 in solution may decrease the solubility of minerals. The influence of dissolved calcite on the solubility of gypsum and anhydrite can be ignored, but dissolved gypsum or anhydrite has a big influence on the calcite solubility. Online calculation is made available on www.geochem-model.org/model.

1. INTRODUCTION

Most geological fluids fall into the system H_2O–CO_2–NaCl–$CaCO_3$–$CaSO_4$ or its subsystems. A thermodynamic model for the calculation of the vapor–liquid–solid (calcite, halite, gypsum, anhydrite) equilibrium coupled with the speciation equilibrium in the liquid phase over a wide range of temperature, pressure and salinity (TPX) is necessary for the calculation of CO_2 solubility, alkalinity, pH, speciation, and mineral solubility under different temperature and pressure or different geological settings. Such model has wide applications in the prediction of the CO_2 destiny in its geological storage, prediction of secondary porosity in oil/gas reservoirs, analyzing fluid inclusions, deducing the formation mechanisms of hydrothermal ore deposits (Giles, 1987; Duan et al., 1995; Duan and Sun, 2003; Pruess and Spycher, 2007).

We have previously (Duan and Li, 2008) presented a thermodynamic model for the quaternary system, H_2O–CO_2–NaCl–$CaCO_3$, which predicts the solubility of CO_2 and calcite and other properties over a wide TPX range.

---

* Corresponding author. Tel.: +86 10 6200 7447; fax: +86 10 6201 0846.

E-mail address: duanzhenhao@gmail.com (Z. Duan).

0016-7037/$ - see front matter © 2011 Elsevier Ltd. All rights reserved.
doi:10.1016/j.gca.2011.05.019

$CaSO_4$ is often another important component in natural aqueous systems (Zanbak and Arthur, 1986; Arslan and Dutt, 1993; Azimi et al., 2007). Addition of $CaSO_4$ to the quaternary system may affect the aqueous chemistry and vapor–liquid–mineral phase equilibrium. In addition to calcite and halite of the quaternary system, gypsum ($CaSO_4 \cdot 2H_2O$) and anhydrite ($CaSO_4$) may precipitate in the quinary system, H_2O–CO_2–NaCl–$CaCO_3$–$CaSO_4$. All these minerals are frequently encountered in sediments or sedimentary rocks. There have been many experimental work on the solubility of gypsum and anhydrite in aqueous solutions and their phase transitions under different temperatures and pressures (Hulett and Allen, 1902; Partridge and White, 1929; Hill, 1937; Booth and Bidwell, 1950; Madgin and Swales, 1956; Dickson et al., 1963; Power and Fabuss, 1964; Blount and Dickson, 1969; Blount and Dickson, 1973), but there is no systematic model to calculate them as a function of temperature, pressure, CO_2 concentration and salinity. As we know, CO_2 sequestration is considered to be a viable way to reduce the CO_2 emission to the air. When injected into the underground, CO_2 will have complex reactions with all the aqueous species. Accurate calculation of the equilibrium of CO_2 with all the possible species, CO_2 solubility, salts solubility, pH values, as well as fluid–rock interactions is very important for the study of the feasibility and security of CO_2 sequestration (Giles, 1987; Pruess and Spycher, 2007; Li et al., 2007). Many researchers have also tried to establish thermodynamic models for this system. For example, Harvie et al. (1984) used Pitzer model to predict mineral solubility in the system Na–K–Mg–Ca–H-Cl-SO_4–OH–HCO_3–CO_3–CO_2–H_2O. The model has good precision, but it is only for 25 °C. Møller (1988), Greenberg and Møller (1989), Christov and Møller (2004a,b) did similar work, but their models did not consider pressure effects, especially partial CO_2 pressure effects, which can be very substantial as can be seen in later sections.

In this work, we established a model for the phase and chemical speciation equilibrium in the CO_2–H_2O–NaCl–$CaCO_3$–$CaSO_4$ system in the temperature range from 25 to 250 °C, and pressure range from 1 to 1000 bar, up to halite saturation. This model takes the following phases and species into account: liquid phase with species H^+, Na^+, Ca^{2+}, $CaHCO_3^+, Ca(OH)^+, OH^-, Cl^-$, HCO_3^-, CO_3^{2-}, HSO_4^-, SO_4^{2-}, $CO_{2(aq)}$, $CaCO_{3(aq)}$ and $CaSO_{4(aq)}$, vapor phase with CO_2 gas and H_2O, and four solid phases, calcite, halite, gypsum and anhydrite.

2. PHENOMENOLOGICAL DESCRIPTION OF THE MODEL

2.1. The establishment of the equilibrium model

In the quaternary system H_2O–CO_2–NaCl–$CaCO_3$, possible phases include vapor, liquid and solids. The vapor phase includes H_2O and CO_2 below 250 °C, and liquid phase may contain the aqueous species H^+, Na^+, Ca^{2+}, $Ca(HCO_3)^+$, $Ca(OH)^+, OH^-$, Cl^-, HCO_3^-, $CO_3^{2-}, CO_{2(aq)}$ and $CaCO_{3(aq)}$ and the solid phase includes calcite and halite. With the addition of $CaSO_4$ into the quaternary system, $CaSO_{4(aq)}$, HSO_4^-, SO_4^{2-} may occur in the liquid phase and anhydrite and gypsum may precipitate as solid phases. For the quinary system, the following independent reactions should be considered

$$H_2O + CO_{2(aq)} \leftrightarrow HCO_3^- + H^+ \tag{1}$$

$$HCO_3^- \leftrightarrow CO_3^{2-} + H^+ \tag{2}$$

$$H_2O \leftrightarrow H^+OH^- \tag{3}$$

$$CaHCO_3^+ \leftrightarrow Ca^{2+} + HCO_3^- \tag{4}$$

$$CaCO_{3(aq)} \leftrightarrow Ca^{2+} + CO_3^{2-} \tag{5}$$

$$Ca(OH)^+ \leftrightarrow Ca^{2+} + OH^- \tag{6}$$

$$H_2O \leftrightarrow H_2O^g \tag{7}$$

$$CO_{2(aq)} \leftrightarrow CO_2^g \tag{8}$$

$$NaCl^s(\text{halite}) \leftrightarrow Na^+ + Cl^- \tag{9}$$

$$CaCO_s^3(\text{calcite}) \leftrightarrow Ca^{2+} + CO_3^{2-} \tag{10}$$

$$HSO_4^- \leftrightarrow H^+ + SO_4^{2-} \tag{11}$$

$$CaSO_{4(aq)}^s \leftrightarrow Ca^{2+} + SO_4^{2-} \tag{12}$$

$$CaSO_4^s(\text{anhydrite}) \leftrightarrow Ca^{2+} + SO_4^{2-} \tag{13}$$

$$CaSO_4 \cdot 2H_2O(\text{gypsum}) \leftrightarrow Ca^{2+} + SO_4^{2-} + 2H_2O \tag{14}$$

When the equilibrium of the whole system reached, for each reaction, we will have:

$$\Delta G_i = \sum_j v_{ij}\mu_{ij} = 0 \tag{15a}$$

where μ_{ij} is the chemical potential, for aqueous species,

$$\mu_{ij} = \mu_{ij}^0 + RT\ln(m_j\gamma_j) \tag{15b}$$

for gas species,

$$\mu_{ij} = \mu_{ij}^0 + RT\ln(x_jP\varphi_j) \tag{15c}$$

and *i* identifies the *i*th reaction; *j* identifies the *j*th species; is stoichiometric coefficient of species *j* in the reaction *i*. μ_{ij}^0 is standard chemical potential at the reference state which is defined in Duan and Li (2008) in detail. Here, m_j is the molality of species *j*. *P* is total vapor pressure. x_j is mole fraction of *j* in vapor phase. γ_j and φ_j are the activity coefficient of species *j* in liquid phase and fugacity coefficient of species *j* in vapor phase, respectively.

The equilibrium constant can be defined as:

$$\ln K_i = -\frac{\sum v_{ij}\mu_{ij}^0}{RT} \tag{16}$$

From (15a), we find that,

$$\ln K_i = \sum \ln a_{ij} \tag{17}$$

K_i is a function of temperature and pressure. From the definition of activity and fugacity, a_{ij} is a function of temperature, pressure and the molality of each species. For a given temperature, pressure and composition, when and only when the equilibrium of the system reaches, the Eq. (17) can be established. After the functions of equilibrium constants and the functions of activity and fugacity coefficients are determined, the Eq. (17) become nonlinear equations of molality of the species, which means the solving of

Table 1
The standard Gibbs free energy (cal/mol), entropy (cal/mol/K) and volume (cm^3/mol) of anhydrite at 25 ° C, 1 bar.*

G_0	S_0	V_0
−315925.0	25.5	45.94

* Helgeson et al. (1978).

Table 2
The parameters of the standard chemical potential of gypsum $\left(\frac{\mu^0}{RT}\right)$ as a function of temperature (K).

a_1	1.35486062d3
a_2	2.26877955d−1
a_3	−6.07006342d4
a_4	−2.27071423d2
a_5	0
a_6	0
a_7	0
a_8	0

the equations is to find out the concentration of species in the liquid and eventually the vapor phase at equilibrium.

2.2. The calculation of equilibrium constant or standard chemical potentials

Duan and Li (2008) has already described the calculation of the equilibrium of the reactions (1)–(10), and here we inherit the results. What we need to do is to find out the equilibrium constants or standard chemical potentials in reactions (11)–(14).

Greenberg and Møller (1989) and Møller (1988) evaluated the standard chemical potentials of anhydrite, gypsum and $CaSO_{4(aq)}$ with solubility data from 25 °C to 250 °C at vapor pressure assuming the chemical potentials of Ca^{2+} and SO_4^{2-} as 0. Here we need to make clear the chemical potentials of aqueous species $Ca^{2+}, SO_4^{2-}, CaSO_{4(aq)}$ and the two salts or the equilibrium constants of the above four reactions. Within the last several decades, many researchers have developed different methods to calculate the equilibrium constants (Ruaya, 1988; Mesmer et al., 1988; Anderson et al., 1991) or the chemical potentials of the species (Helgeson, 1969; Sverjensky et al., 1997). The HKF model, developed by Helgson and his co-workers (Helgeson, 1969; Helgeson and Kirkham, 1976; Helgeson et al., 1981), permits calculation of standard partial molal thermodynamic properties of aqueous ions to 600 °C and 5 kb. Shock and Helgeson (1988), Shock et al. (1992), Sverjensky et al. (1997) and Tanger and Helgeson (1988) developed a more accurate model on the basis of the HKF model, called revised HKF model. With the revised HKF model, the standard thermodynamic properties of hundreds of aqueous species can be calculated.

Helgeson and co-workers developed a software package, SUPCRT92, which calculates the standard thermodynamic properties. Johnson et al. (1992) introduced the software and summarized the revised HKF model.

The apparent standard molal Gibbs free energy of the jth aqueous solute species can be expressed as follows:

$$\begin{aligned}
G^0_{j,P,T} - G^0_{j,P_r,T_r} = {} & -S^0_{j,Pr,T_r}(T-T_r) - c_{1,j}\left[T\ln\left(\frac{T}{T_r}\right) - T - T_r\right] \\
& + a_{1,j}(P-P_r) + a_{2,j}\ln\left(\frac{\Psi+P}{\Psi+P_r}\right) \\
& - c_{2,j}\left\{\left[\left(\frac{1}{T-\Theta}\right) - \left(\frac{1}{T_r-\Theta}\right)\right]\right. \\
& \times \left.\left[\frac{\Theta-T}{\Theta}\right] - \frac{T}{\Theta^2} ln\left[\frac{T_r(T-\Theta)}{T(T_r-\Theta)}\right]\right\} \\
& + \left(\frac{1}{T-\Theta}\right)\left[a_{3,j}(P-P_r) + a_{4,j}\ln\left(\frac{\Psi+P}{\Psi+P_r}\right)\right] \\
& - \omega_j(Z+1) + \omega_{j,P_r,T_r}(Z_{P_r,T_r}+1) \\
& + \omega_{j,P_r,T_r} Y_{P_r,T_r}(T-T_r) \qquad (18)
\end{aligned}$$

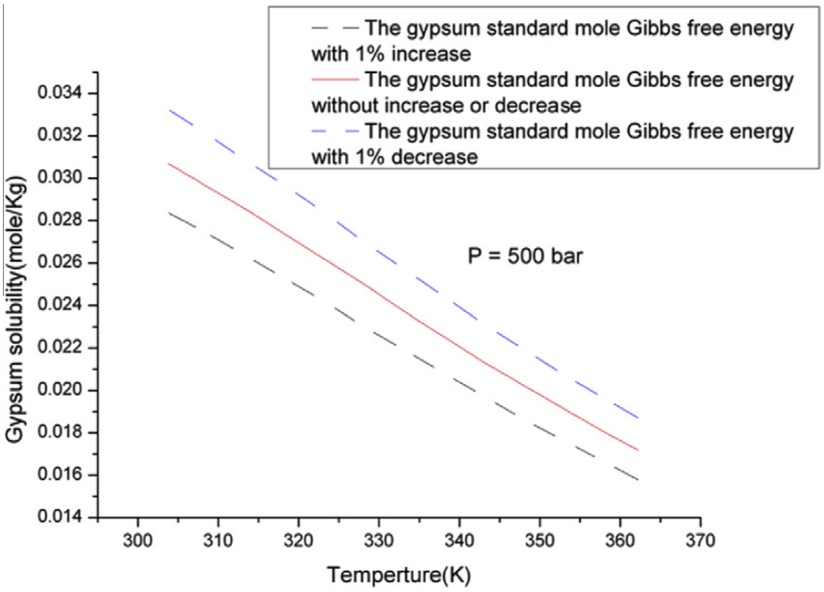

Fig. 1. Gypsum solubility calculated from standard Gibbs free energy, showing that 1% of change of standard free energy can cause 10% of variation in mineral solubility.

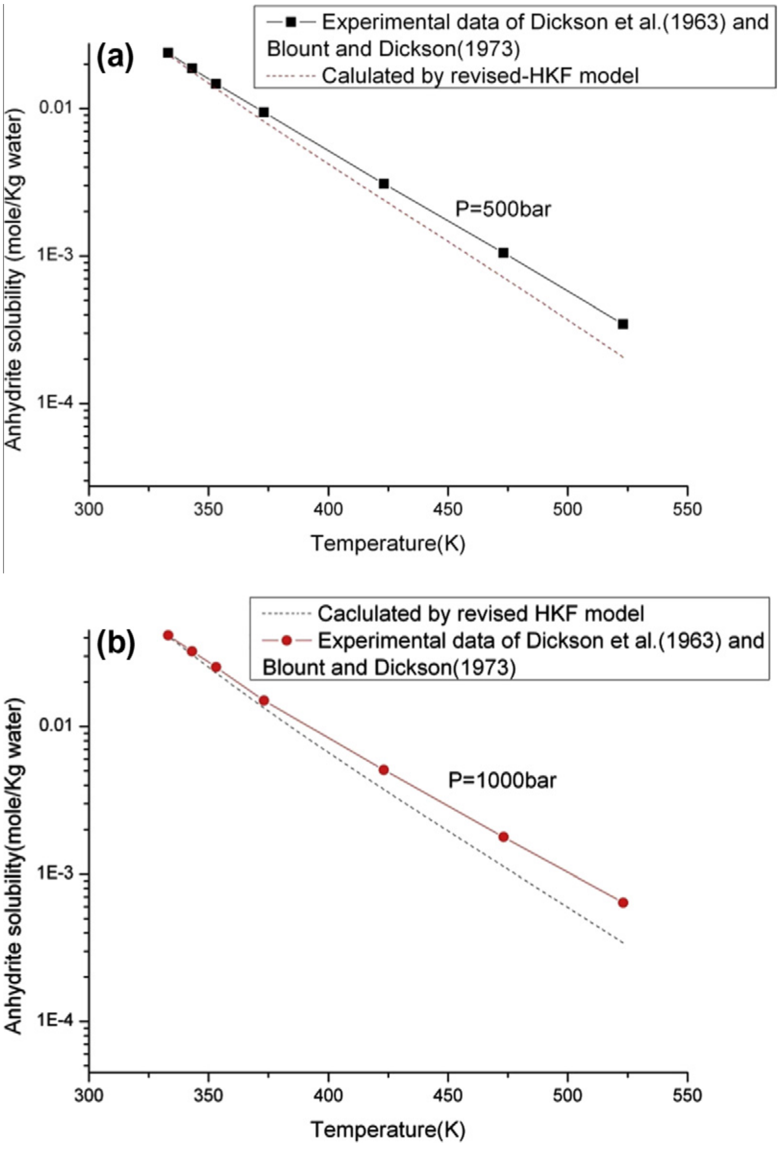

Fig. 2. A comparison of the calculated anhydrite solubility from the revised HKF model with experimental results.

Here, P_r,T_r stand for the reference pressure and temperature (1 bar and 25 °C here); S^0_{j,P_r,T_r} denotes standard molal entropy at reference state; Θ and Ψ refer to solvent parameters equal to 228 K and 2600 bars, respectively; ω_j is conventional Born coefficient of the species j; Y and Z are solvent Born functions; $a_{1\ldots4,j}$ denote equation-of-state coefficients unique to the jth aqueous solute species. $c_{1\ldots2,j}$ stand for P/T-independent adjustable regression parameters unique to the jth aqueous solute species.

Table 3
The parameters of additional term of standard chemical potential of gypsum and anhydrite as a function of temperature (K) and pressure (bar).

	Gypsum	Anhydrite
a_1	−.959732931546D+03	0.685503896814D+04
a_2	−.138483395432D+01	0.554032946200D+01
a_3	0.272816804474D−03	0.341549716317D+01
a_4	0.285458724885D+01	0.833551833463D−02
a_5	0.375456113109D−02	−.141330606017D+04
a_6	−.403407381449D−06	−.139693530948D+01
a_7	–	0.953551522365D+05
a_8	–	−.100216355361D+03

The apparent standard molal Gibbs free energy and enthalpy of formation of a mineral can be expressed as follows:

$$\begin{aligned} G^0_{P,T} - G^0_{P_r,T_r} = & -S^0_{Pr,T_r}(T - T_r) \\ & + \sum_{i=1}^{1+\phi_T} a_i \left[T_{i+1} - T_i - T_{i+1} \ln \left(\frac{T_i + 1}{T_i} \right) \right] \\ & + \sum\nolimits_{i=1}^{1+\phi_T} \left\{ \frac{(-c_i - b_i T_{i+1} T_i^2)(T_{i+1} - T_i)^2}{2 T_{i+1} T_i^2} \right\} \\ & + V^0_{P_r,T}(P - P_r) - \sum_{i=1}^{\phi_P} \int_{P_{t_j},T}^{P} \Delta V^0_{t_j} dP \\ & - \sum\nolimits_{i=1}^{\phi T} \frac{\Delta H^0_{t_i}}{T_{\ \ t_i}} (T - T_{t_i}) \end{aligned} \tag{19}$$

Table 4
The Pitzer parameters for sulphate.

$\beta^{(0)}_{Ca-SO_4}$	This study
$\beta^{(1)}_{Ca-SO_4}, \beta^{(2)}_{Ca-SO_4}, C^{\varphi}_{Ca-SO_4}, \beta^{(0)}_{Na-SO_4}, \beta^{(1)}_{Na-SO_4}, C^{\varphi}_{Ca-SO_4}$	Møller (1988), Greenberg and Møller (1989)
$\beta^{(0)}_{Ca-HSO_4}, \beta^{(1)}_{Ca-HSO_4}, C^{\varphi}_{Ca-HSO_4}$	Christov and Møller (2004b)
$\beta^{(0)}_{Na-HSO_4}, \beta^{(1)}_{Na-HSO_4}, C^{\varphi}_{Na-HSO_4}, \beta^{(0)}_{H-SO_4}, \beta^{(1)}_{H-SO_4}$	Christov and Møller (2004a)
$C^{\varphi}_{H-SO_4}, \beta^{(0)}_{H-HSO_4}, \beta^{(1)}_{H-HSO_4}, C^{\varphi}_{H-HSO_4}$	
$\theta_{SO_4-OH}, \theta_{SO_4-HSO_4}, \theta_{HSO_4-Cl}, \theta_{HSO_4-Cl}$	Christov and Møller (2004a)
θ_{SO_4-Cl}	Møller (1988)
$\Psi_{Na,H,SO_4}, \Psi_{Na,H,HSO_4}, \Psi_{H,SO_4,HSO_4}, \Psi_{Na,SO_4,HSO_4}$	Christov and Møller (2004a,b)
$\Psi_{H,Cl,SO_4}, \Psi_{H,Cl,HSO_4}, \Psi_{Na,Cl,HSO_4}, \Psi_{Ca,H,SO_4}$	
$\Psi_{Ca,HSO_4,SO_4}, \Psi_{Ca,SO_4,OH}, \Psi_{Ca,Cl,HSO_4}, \Psi_{Na,Cl,HSO_4}$	
$\Psi_{Ca,Cl,SO_4}, \Psi_{Na,Cl,SO_4}, \Psi_{Ca,Na,SO_4}, \Psi_{Cl,SO_4,Ca}$	Greenberg and Møller (1989), Møller (1988)
$\lambda_{CO_2-SO_4}, \lambda_{CO_2-HSO_4}$	This study
$\lambda_{CO_2-CaSO_4}$	Set to 0

Table 5
The Pitzer parameter $\beta^{(0)}_{CaSO_4}$ as function of temperature (K) and pressure (bar).

a_1	−.529591713285D+01
a_2	0.103294514294D−02
a_3	−.419956309165D−05
a_4	0.550380707079D−02
a_5	0.400012224741D−04
a_6	0.170762887873D−07
a_7	0.121302564389D+04
a_8	−.491824288014D+01

Here, ϕ_T stands for the number of phase transitions from P_r, T_r to P_r, T, ϕ_P denotes the number of phase transitions from P_r,T to P, T; $\Delta V^0_{t_j}, \Delta H^0_{t_j}$, represents the change in standard molal volume and enthalpy associated with the jth of the total phase transitions, respectively; a_i,b_i,c_i are the parameters. In the SUPCRT92 database, the parameters, $a_1, a_2, a_3, c_1, c_2, \omega_{j,P_r,T_r}, S^0_{j,P_r,T_r}, G^0_{P_r,T_r}$ and some other properties of hundreds of aqueous species and minerals are given.

In this work, the standard chemical potentials of $Ca^{2+}, SO_4^{2-}, CaSO_{4(aq)}$ and anhydrite are calculated based on the revised HKF model. The standard Gibbs free energy, entropy and volume of anhydrite are listed in Table 1. However, the parameters of gypsum are not available, and they must be evaluated in this study.

Møller (1988) gave a fitting equation of standard chemical potential of gypsum at vapor pressure from 25 °C to 110 °C, as a function of T:

$$\frac{\mu^0_M}{RT} = a_1 + a_2T + \frac{a_3}{T} + a_4 \ln T + \frac{a_5}{T-263} + a_6T^2 + \frac{a_7}{680-T} + \frac{a_8}{T-227} \qquad (20)$$

where, a_1–a_8 are parameters as listed in Table 2. In the model of Møller (1988), the standard chemical potentials of the ionic species OH^-, Ca^{2+}, SO_4^{2-} were set equal to zero, and the temperature dependent standard chemical potential μ^0_{M,H_2O} established by Busey and Mesmer (1978) was applied. The subscript M of μ^0_M and μ^0_{M,H_2O} stands for the Møller standard. Therefore, in this work, the chemical potential of gypsum should be $\mu^0(T) = \mu^0_M(T) + \mu^0_{Ca^{2+}} + \mu^0_{SO_4^{2-}}$, and the chemical potential of H_2O should be $\mu^0_{H_2O} = \mu^0_{M,H_2O} + \mu^0_{OH^-}$.

In thermodynamics, we have

$$\left(\frac{\partial \mu^0}{\partial P}\right)_T = \overline{V}^0 \qquad (21)$$

$$\left(\frac{\partial \overline{V}^0}{\partial P}\right) = -\bar{\kappa}^0 \qquad (22)$$

where $\overline{V}^0$ is the partial molar volumes, and $\bar{\kappa}^0$ is the standard partial molar compressibility. Now we can get the second approximation about pressure of the standard chemical potential of gypsum.

$$\mu^0(T,P) = \mu^0(T,P_s) + \overline{V}^0(P-P_s) - 0.5\bar{\kappa}^0(P-P_s)^2 \qquad (23)$$

Here, P_s is 1 bar below 100 °C, and is vapor pressure above 100 °C. Millero (1982) analyzed the effect of pressure on the solubility of minerals in water and seawater based on experimental partial molal volume and compressibility of different aqueous species and minerals. Millero (1982) gave an empirical relation $\overline{V}^0$ and $\bar{\kappa}^0$ of minerals,

$$\bar{\kappa}^0 = \overline{V}^0\beta_s \qquad (24)$$

From Fig. 2 in Millero (1982), β_s for gypsum can be estimated at 2.13×10^{-6}. β_s is so small that the third term of the right hand side in Eq. (23) can be ignored.

The accuracy of equilibrium constant is very important for the calculation of the mineral solubility. One percent of difference may make a difference of ten percent in salt solubility. From Fig. 1, we can find that at 500 bar with 1% increase or decrease of equilibrium constant, there will be 10% decrease or increase in the gypsum solubility. As we know, the solubility of gypsum or anhydrite in water is very small, and the saturate solution is nearly ideal, so there is little effect on adjusting activity coefficient parameters. The standard mole Gibbs free energy calculated using Eqs. (18)–(20), (23) is not accurate enough to describe the solubility of gypsum and anhydrite, even though there is only a few percent of uncertainty. Fig. 2 shows that as temperature increases, there will be an increasing error of anhydrite solubility if calculated with the revised HKF model without any additional revision.

Here, we make an adjustment on the salt standard Gibbs free energy. Set the standard Gibbs free energy of anhydrite, $\mu^{(0)}_{anh} = \mu^{0*}_{anh} + \varepsilon$, where μ^{0*}_{anh} is the standard Gibbs free

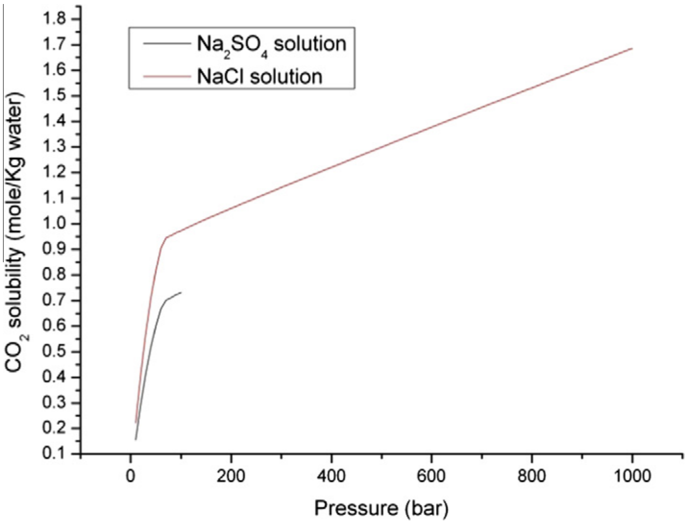

Fig. 3. Comparison of CO_2 solubility in NaCl solution and Na_2SO_4 solution under pressures blow 100 bar at temperature 298.15 K.

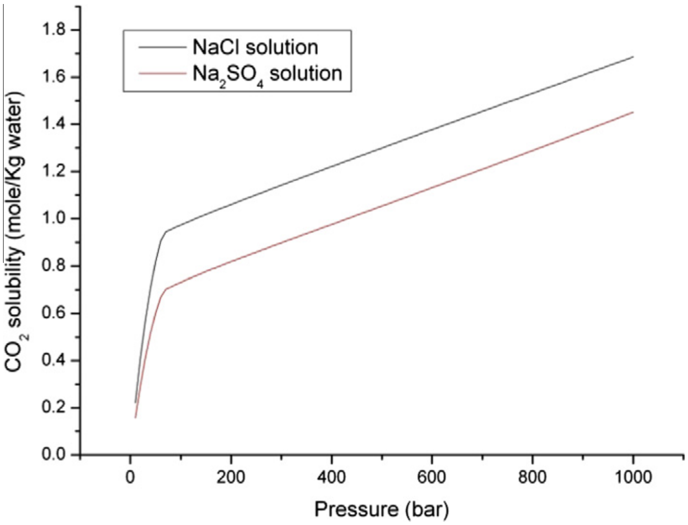

Fig. 4. CO_2 solubility in NaCl solution and estimated CO_2 solubility in Na_2SO_4 solution under pressures from 1 to 1000 bar at 298.15 K.

Table 6
The neutral-ion parameters of CO_2.

	$2\lambda_{CO_2-Na} + 2\lambda_{CO_2-SO_4}$
a_1	−.129486118638D+00
a_2	0.815387805594D−04
a_3	0.158499586915D+03
a_4	−.887125993018D−01
a_5	0.614784284629D−01
a_6	−.159049335240D−04

The fitting equation is: Parameter $(T,P) = a_1 + a_2T + \frac{a_3}{T} + \frac{a_4P}{T} + \frac{a_5P}{630-T} + a_6T\ln P$.
Note: In this study, we set $\lambda_{CO_2-SO_4} = 2\lambda_{CO_2-HSO_4}$.

energy calculated above for anhydrite, ε is the adjusted value, which is a function of temperature and pressure and can be fitted using the experimental solubility data of Dickson and co-workers (1963; Blount and Dickson, 1969; Blount and Dickson, 1973). The fitting equation is as follows:

$$\varepsilon(T,P) = a_1 + a_2P + a_3T + a_4PT + a_5\log(T) + a_6P\ \log(T) + \frac{a_7}{647.0-T} + \frac{a_8P}{647.0-T} \tag{25}$$

$a_1 - a_8$ are parameters, and the *TP* range is 25–250 °C, 1–1000 bar.

Gypsum standard chemical potential is treated in the same way, but the fitting equation is as following:

$$\varepsilon'(T,P) + a_1 + a_2P + a_3P^2 + a_4T + a_5TP + a_6TP^2 \tag{26}$$

The *TP* range is 25–100 °C, 1–1000 bar.

The values of the parameters are given in Table 3.

The parameters of HSO_4^- are obtained from SUPCRT92 database. The equilibrium constant of the reaction (11) can also be calculated by the revised HKF model.

2.3. Calculation of activities of species in aqueous solution (liquid phase)

As discussed above, equilibrium constants can be used to calculate speciation equilibrium in ideal solution. However, as the concentration of aqueous species increases, the solution departs away from ideal states. The non-ideal properties can be expressed by activity coefficient for aqueous species, fugacity coefficient for vapor species and osmotic coefficient for H_2O.

Since 1973, Pitzer and co-workers established a specific interaction model which can estimate the activity coefficients of aqueous species and osmotic coefficient of water in solutions up to high concentrations (Pitzer, 1973; Pitzer

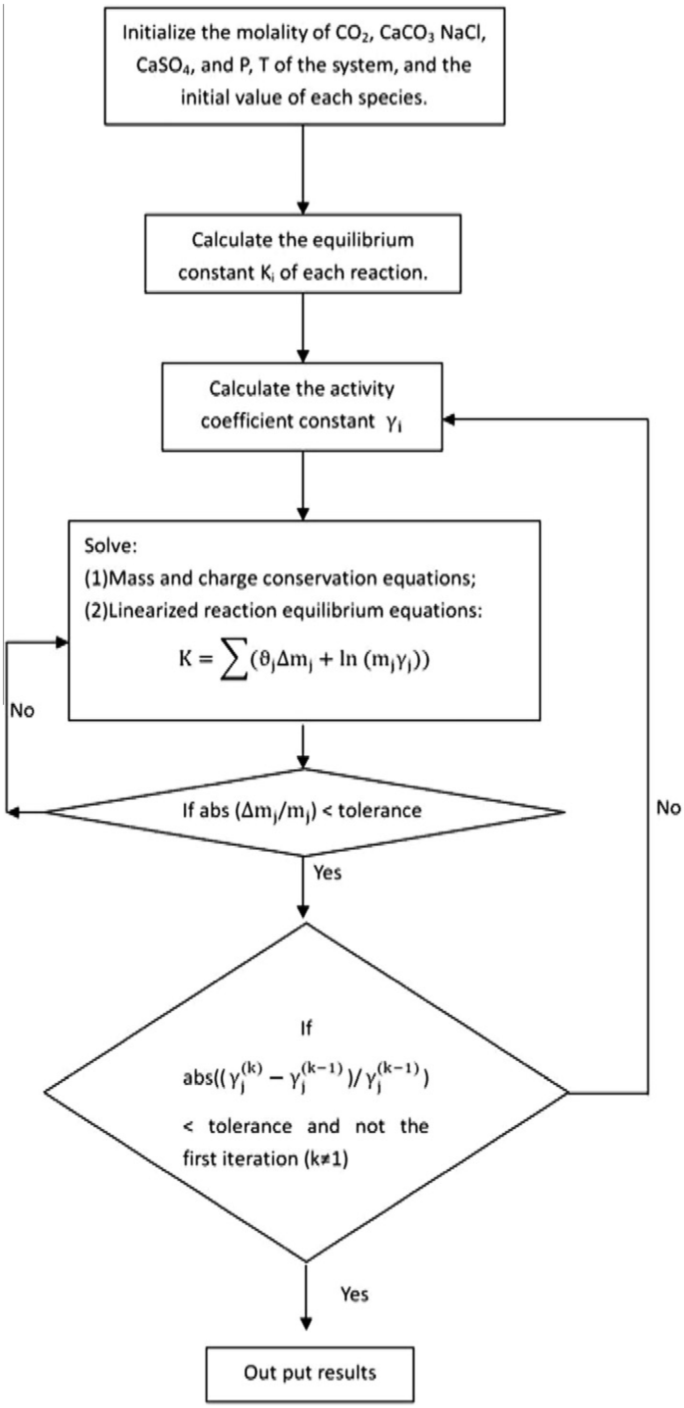

Fig. 5. The flow chart of the algorithm for the equilibrium calculation.

and Mayorga, 1973; Pitzer and Kim, 1974). Within the last forty years, many researchers used this model to calculate activity coefficient within wide temperature and pressure variation in high concentrated electrolytic solutions successfully (Harvie and Weare, 1980; Harvie et al., 1984; Møller, 1988; Christov and Møller, 2004a,b; Li and Duan,

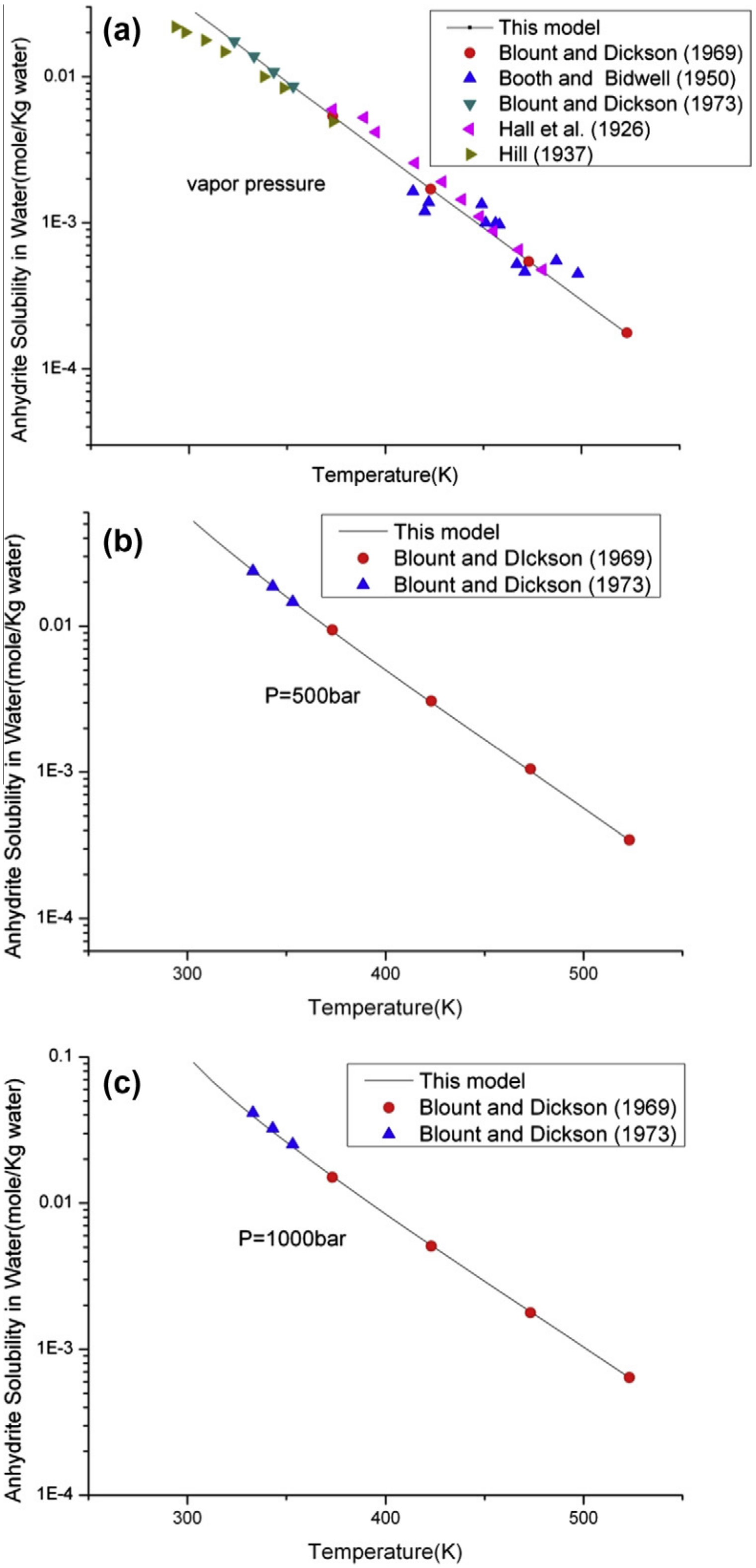

Fig. 6. A comparison of the calculated anhydrite solubility in water from the model with the experimental data.

2007; Duan and Li, 2008). Here, we also use Pitzer model to calculate the activity coefficients and osmotic coefficient. The formulas of Pitzer model are list in the appendix.

The Pitzer parameters for the system H_2O–CO_2–NaCl–$CaCO_3$ have been given in the study of Duan and Li (2008). In this study, we need to determine the sulfate

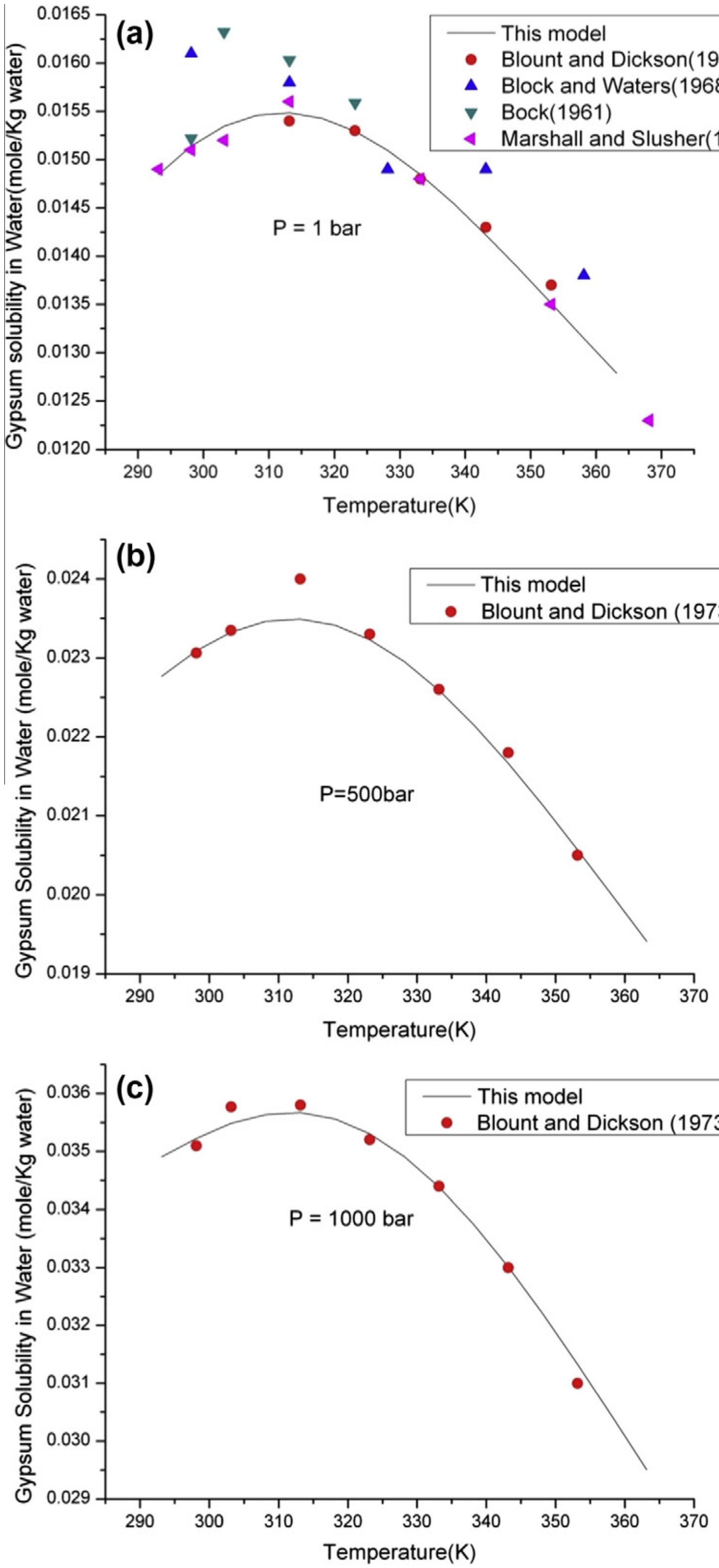

Fig. 7. A comparison of calculated gypsum solubility in water from the model with the experimental data.

related Pitzer parameters (Table 4). Firstly, we determine the virial coefficients of Ca^{2+} and SO_4^{2-}, $\beta^{(0)}_{CaSO_4}$ from the gypsum and anhydrite solubility data in water and solution (Blount and Dickson, 1969, 1973), with the fitting equation as follows:

$$\beta^{(0)} = a_1 + a_2P + a_3P^2 + +a_4T + a_5TP + a_6TP^2 + \frac{a_7}{647.0 - T} + \frac{a_8P}{647.0 - T} \tag{27}$$

Table 5 shows the value of the parameters in Eq. (27). $\beta^{(1)}_{CaSO_4}, \beta^{(2)}_{CaSO_4}$, and $C^{\varphi}_{CaSO_4}$ were determined by Møller (1988) and Greenberg and Møller (1989), and we adapted them here. $\beta^{(1)}_{CaSO_4}$ has the constant value 3.0. $\beta^{(2)}_{CaSO_4}$ equals $-129.399287 + 0.400431027T$. $C^{\varphi}_{CaSO_4}$ is set to be zero.

The parameters $\beta^{(0)}_{Ca,Cl}, \beta^{(1)}_{Ca,Cl}$, $\beta^{(0)}_{Na,SO_4}$, $\beta^{(1)}_{Na,SO_4}, C^{\varphi}_{Na,SO_4}$, $\theta_{Cl,SO_4}, \theta_{Na,Ca}$, $\Psi_{Cl,SO_4,Na}, \Psi_{Cl,SO_4,Ca}$, Ψ_{Ca,Cl,SO_4}, $\Psi_{Na,Ca,Cl}$ and Ψ_{Na,Ca,SO_4} are adapted from Møller (1988), and the parameter $C^{\varphi}_{Ca,Cl}$ is adapted from Greenberg and Møller (1989).

The Pitzer parameters of CO_2 interaction with other species should also be evaluated. Experimental data of CO_2 solubility in $CaSO_4$ solution is scarce, so we have to evaluate the Pitzer parameters in an indirect way. Bermejo et al. (2005) studied the influence of Na_2SO_4 on the CO_2 solubility in water experimentally up to 100 °C, and more than 140 bars. Rumpf and Maurer (1993) measured the solubility of CO_2 in aqueous Na_2SO_4 solutions (1 and 2 mole Na_2SO_4/Kg water) in temperature range from 313 to 433 K and pressure up to 100 bars. The pressure of the data is not high enough for the modeling. As we know, the variation of CO_2 solubility in salt solution of different kinds with temperature and pressure has similarity to some extent as we have proved previously (Duan and Sun, 2003). So, we consider that at a given temperature the solubility variation of

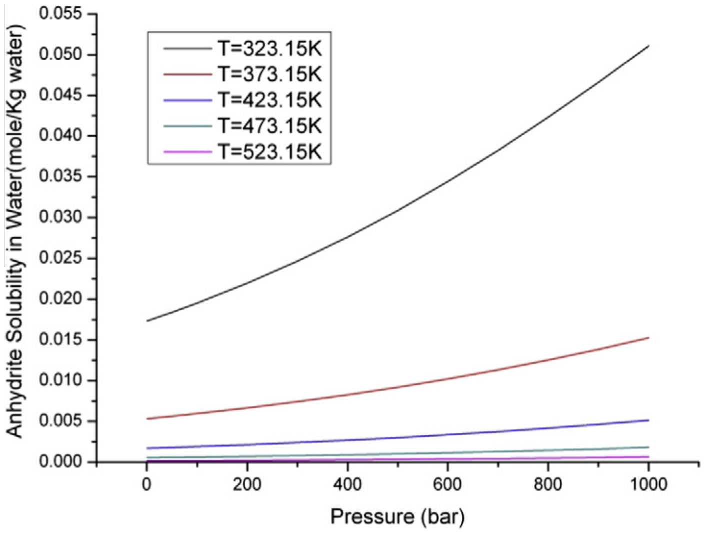

Fig. 8. Anhydrite solubility varying with pressure at different temperatures.

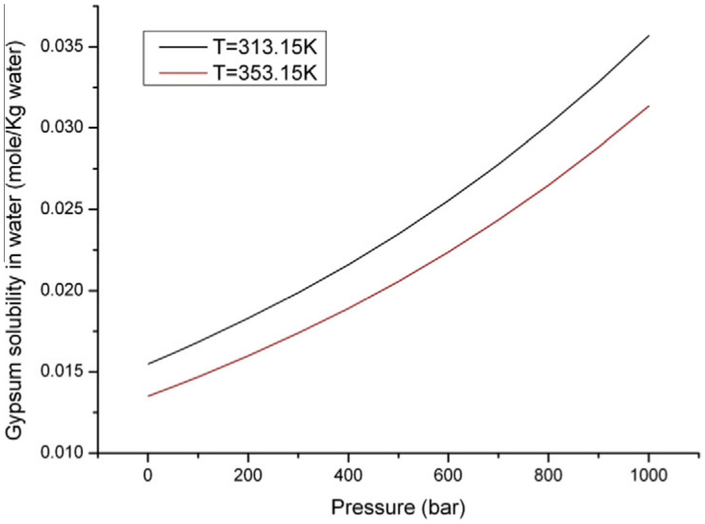

Fig. 9. Gypsum solubility varying with pressure at different temperatures.

CO_2 in Na_2SO_4 solution with pressure has the similar curve shape of the NaCl solution (Fig. 3). At temperature 298.15 K and $mNaCl = mNa_2SO_4 = 1$ m, either in NaCl solution or in Na_2SO_4 solution, the CO_2 solubility increases quickly before 71 bar and then level off. We assume that the slope of CO_2 solubility variation in Na_2SO_4 solution above

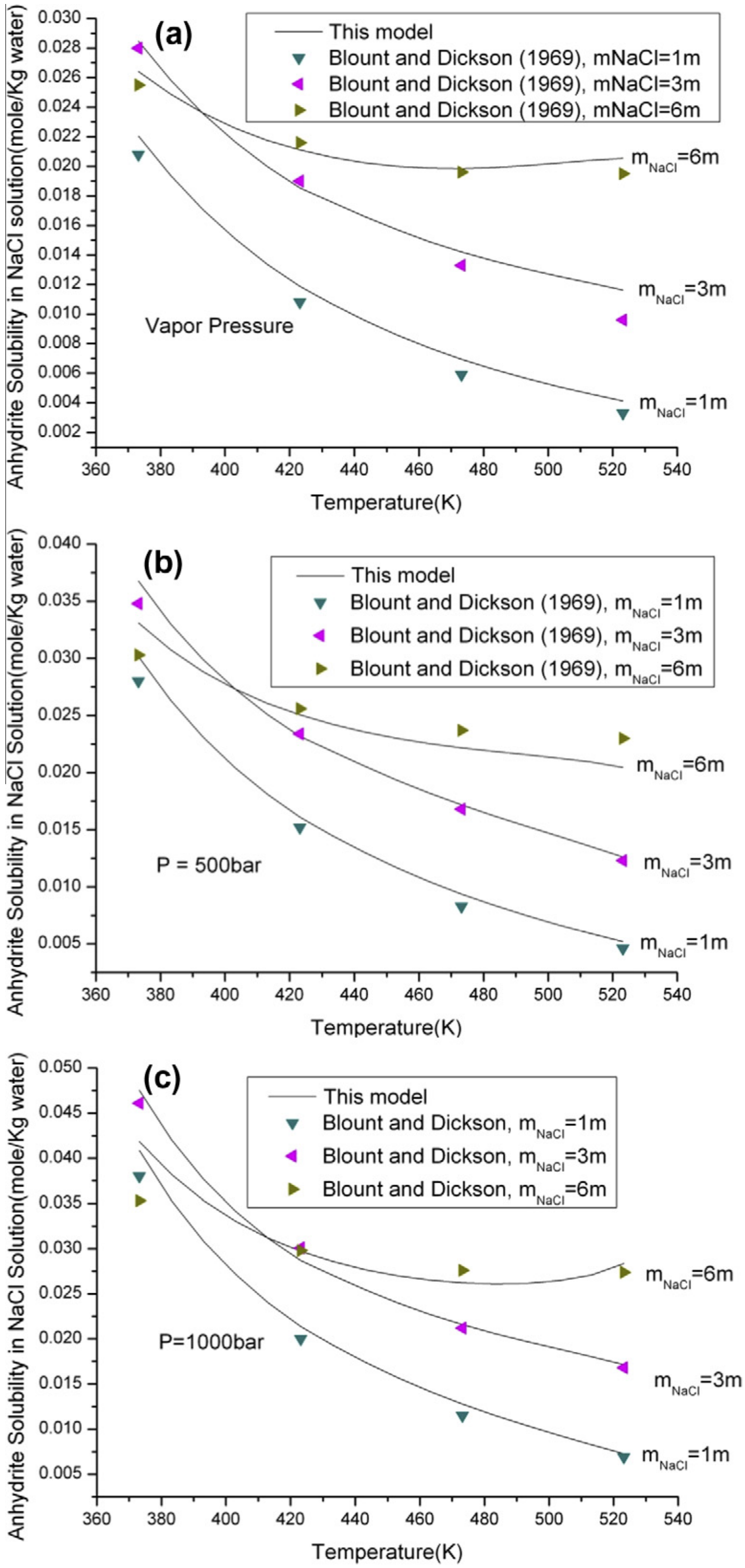

Fig. 10. Comparison of the calculated anhydrite solubility in NaCl solution with experimental data (Blount and Dickson, 1969).

71 bar is the same with the slope NaCl in solution. In this way, the solubility data can be expanded. See Fig. 4. We expand the data for other temperatures ($T = 323.15$ K, 373.15 K, 423.15 K).

With the experimental data and the expanded data, the Pitzer parameter $2\lambda_{CO_2-Na} + \lambda_{CO_2-SO_4}$ is evaluated. The solubility can be calculated with the accuracy within 5%. The results are listed in Table 6. Duan and Sun (2003) evaluated the Pitzer parameter λ_{CO_2-Na} using the solubility data, and can predict the CO_2 solubility precisely in NaCl solution to high ionic strength. So the Pitzer parameter $\lambda_{CO_2-SO_4}$ can be calculated.

2.4. Algorithm description

All the phase and speciation equilibrium in the system H_2O–CO_2–NaCl–$CaCO_3$– $CaSO_4$ can be represented by reactions (1)–(14). When the system reaches equilibrium, the equations. (15) and (17) must be satisfied. Once the standard chemical potentials or equilibrium constants and the related Pitzer parameters are evaluated at a given temperature and pressure, the phases and concentrations of the species in each phase can be obtained by solving these nonlinear equations. For details, see Fig. 5.

3. THE PREDICTION OF VARIOUS PROPERTIES USING THE MODEL

After the model is established, the phase and speciation equilibrium can be calculated easily at a given temperature and pressure. In other words, we can find what phase occurs and in each fluid phase what species exists and how much. Therefore, the model can be used to calculate CO_2 solubility in H_2O–NaCl–$CaCO_3$–$CaSO_4$ solution, the solubility of anhydrite, gypsum, calcite, halite, alkalinity, pH value as a function of temperature, pressure and salinity.

3.1. The solubility of the minerals

As we introduced above, there are four kinds of salts (halite, calcite, gypsum and anhydrite) are included in the system under the $T - P$ conditions considered, and the solubility of the salts in water or in H_2O–CO_2–NaCl–$CaCO_3$–$CaSO_4$ solutions can be predicted.

3.1.1. Anhydrite and gypsum solubility

Many researchers reported the calcium sulphate mineral (anhydrite and gypsum) solubility at 100 °C and below at 1 bar in last century (Hulett and Allen, 1902; Melcher, 1910; Hill, 1937; Posnjak, 1938; Madgin and Swales, 1956; Bock, 1961; Denman, 1961; Power and Fabuss, 1964; Zen, 1965; Power et al., 1966). Some studies were carried out for temperatures above 100 °C and at saturation pressure of the solution (Melcher, 1910; Hall et al., 1926; Partridge and White, 1929; Straub, 1932; Booth and Bidwell, 1950; Power and Fabuss, 1964; Marshall et al., 1964). Some measurements were done under supercritical conditions by Morey and Hesselgesser (1951) and Styrikovich and Khokhlov (1957). Dickson et al. (1963) did a systematic study of anhydrite solubility in H_2O at pressures above the vapor pressure of the solutions.

Many researchers measured the gypsum and anhydrite solubilities in the $CaSO_4$–NaCl–H_2O system at 25–200 °C, and at 1 bar or the saturation pressure with NaCl up to halite saturation. Bock (1961), D'Ans et al. (1955), Madgin and Swales (1956), Marshall and Slusher (1966), Power and Fabuss (1964) and Power et al. (1966) did the experiment at 100 °C and 1.01325 bar. Marshall et al. (1964) studied the $CaSO_4$–NaCl–H_2O system at temperatures from 40 to 200 °C, 0–4 m NaCl molality. Hardie (1967) and Zen (1965) studied the reliability of anhydrite solubility measurements below 70 °C. Blount and Dickson (1969) did an extensive experimental study of $CaSO_4$–NaCl–H_2O system from 100 °C to 450 °C and 1–1000 bar, with NaCl molality up to more than 6 m.

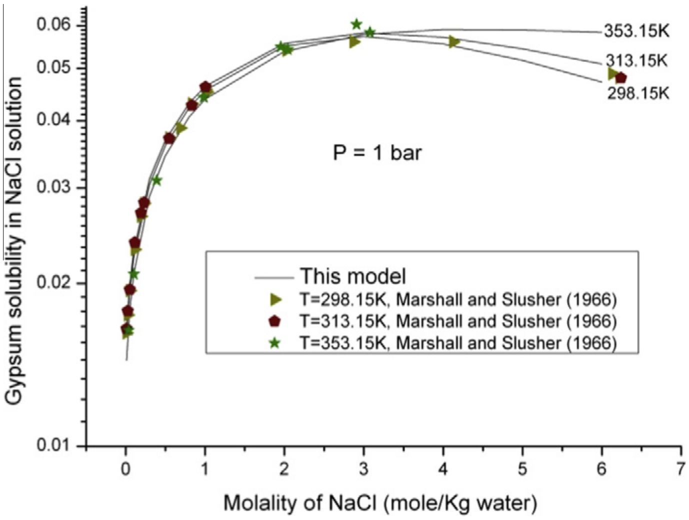

Fig. 11. Comparison of the calculated gypsum solubility in NaCl solution with experimental data (Marshall and Slusher, 1966).

Blount and Dickson (1973) extensively analyzed the experimental solubility data of gypsum and anhydrite in water and in NaCl solutions. They used the data given by Dickson and co-workers to study four-phase equilibrium, anhydrite, gypsum, saturated solution, and vapor. They gave the four phase invariant point which was thought to

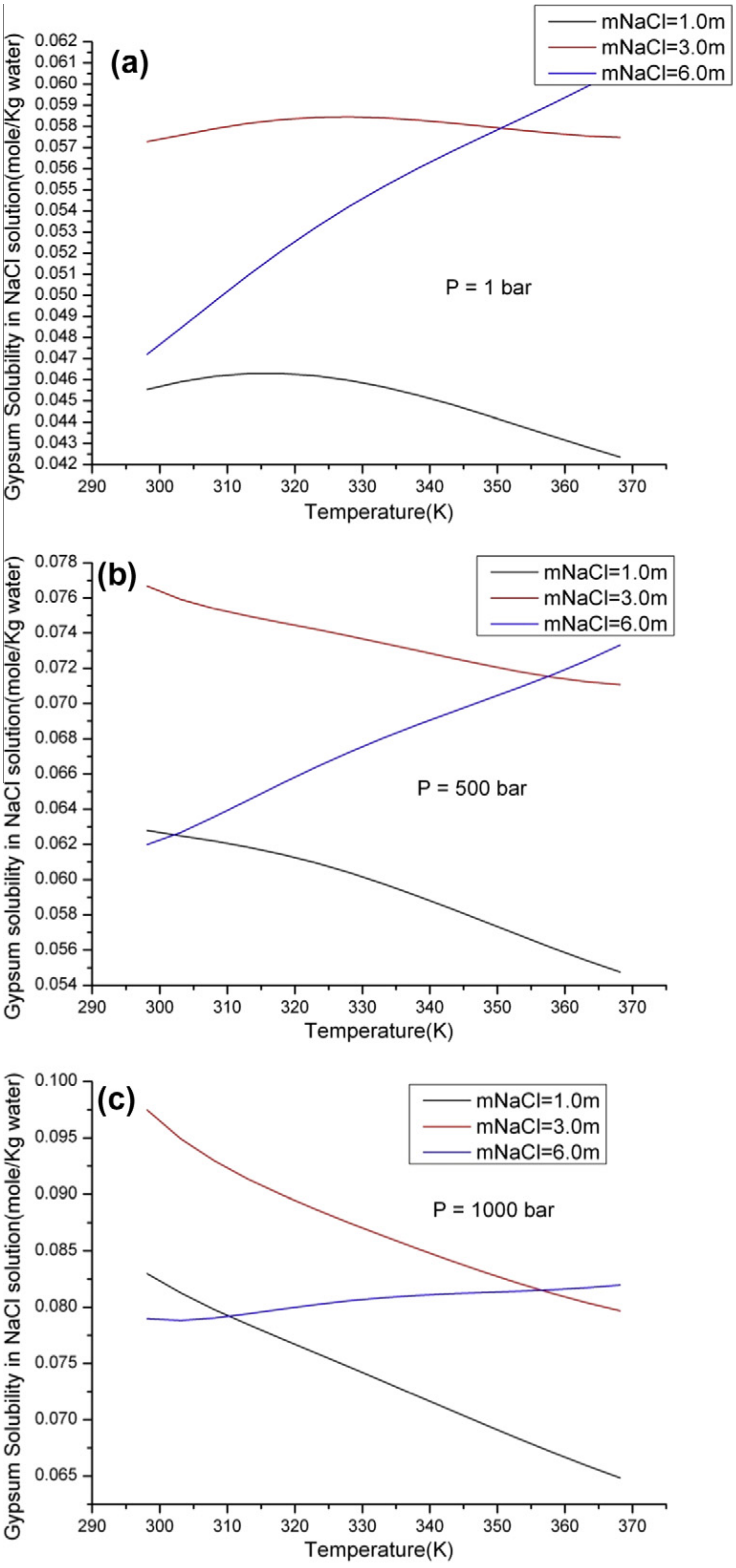

Fig. 12. Calculated gypsum solubility in NaCl solutions as a function of temperature, pressure and NaCl molality.

be the most reliable and acceptable. Zanbak and Arthur (1986) pointed out that Blount and Dickson's experiments had been carried out reversibly and been repeatable. In this work, Dickson and co-workers' data are adopted for the evaluation of the parameters in the model.

With the model in this work, we can calculate anhydrite and gypsum solubility in water. From Figs. 6 and 7, we can find that the calculated anhydrite and gypsum solubility are compatible with the experimental data. For anhydrite, the solubility decreases with the increase of temperature at a given pressure. For gypsum, the solubility first increases and then decreases with temperature at a given pressure, and the turning point is in a neighborhood of 40 °C. From Figs. 8 and 9, we can see that increasing

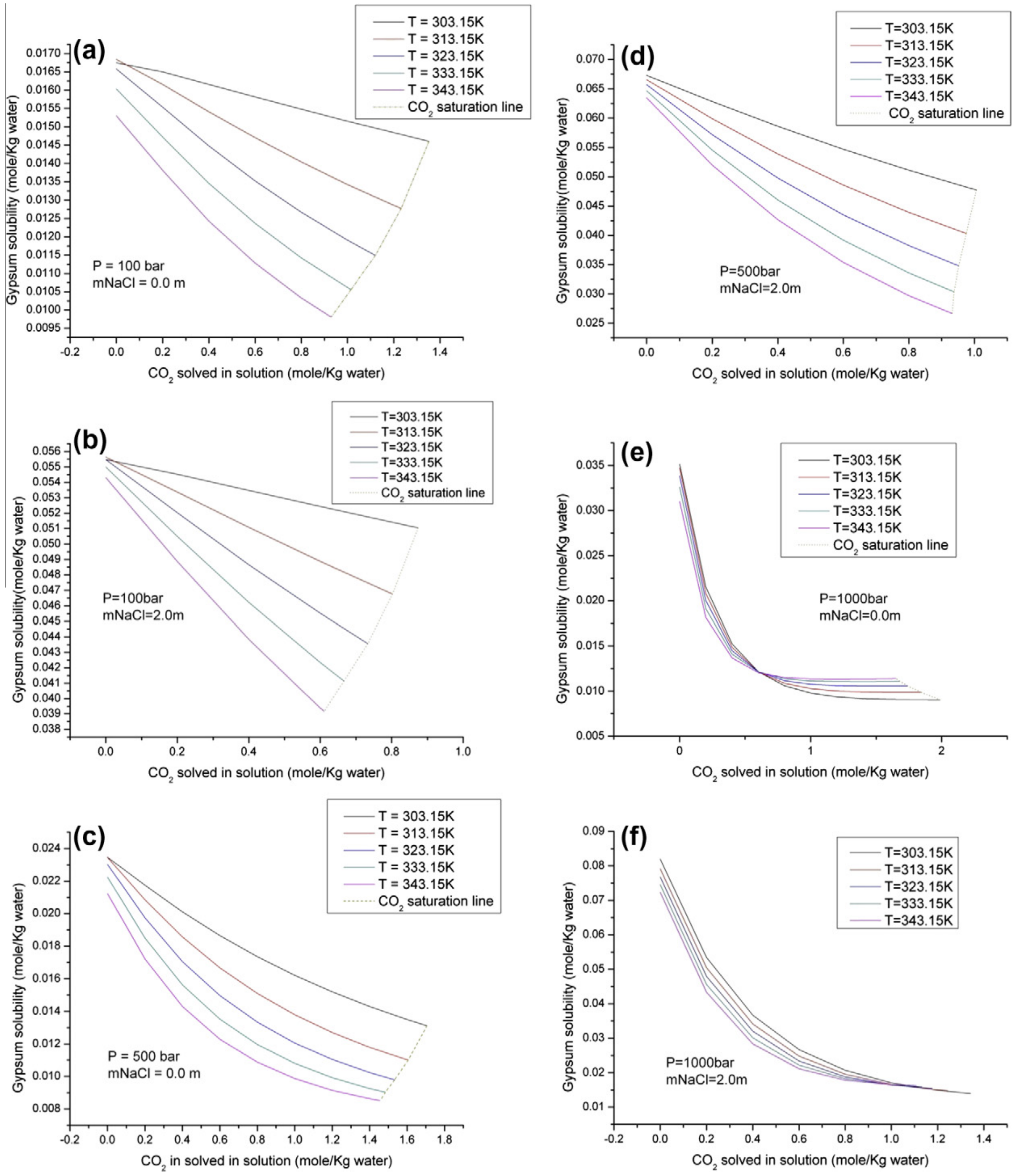

Fig. 13. Gypsum solubility varying with CO_2 molality. (a) $P = 100$ bar, m_{NaCl} (NaCl molality) = 0; (b) $P = 100$ bar, $m_{NaCl} = 2.0$ m; (c) $P = 500$ bar, $m_{NaCl} = 0$; (d) $P = 500$ bar, $m_{NaCl} = 2.0$ m; (e) $P = 1000$ bar, $m_{NaCl} = 0$; (f) $P = 1000$ bar, $m_{NaCl} = 2.0$ m.

pressure can substantially increase the solubility of both anhydrite and gypsum.

This model can also predict the anhydrite and gypsum solubility in NaCl solutions up to NaCl concentration reaching halite saturation without fitting the experimental data when the model is constructed. Compared with experimental data (Blount and Dickson, 1973), the model predicts anhydrite solubility within the 10% of deviation. The

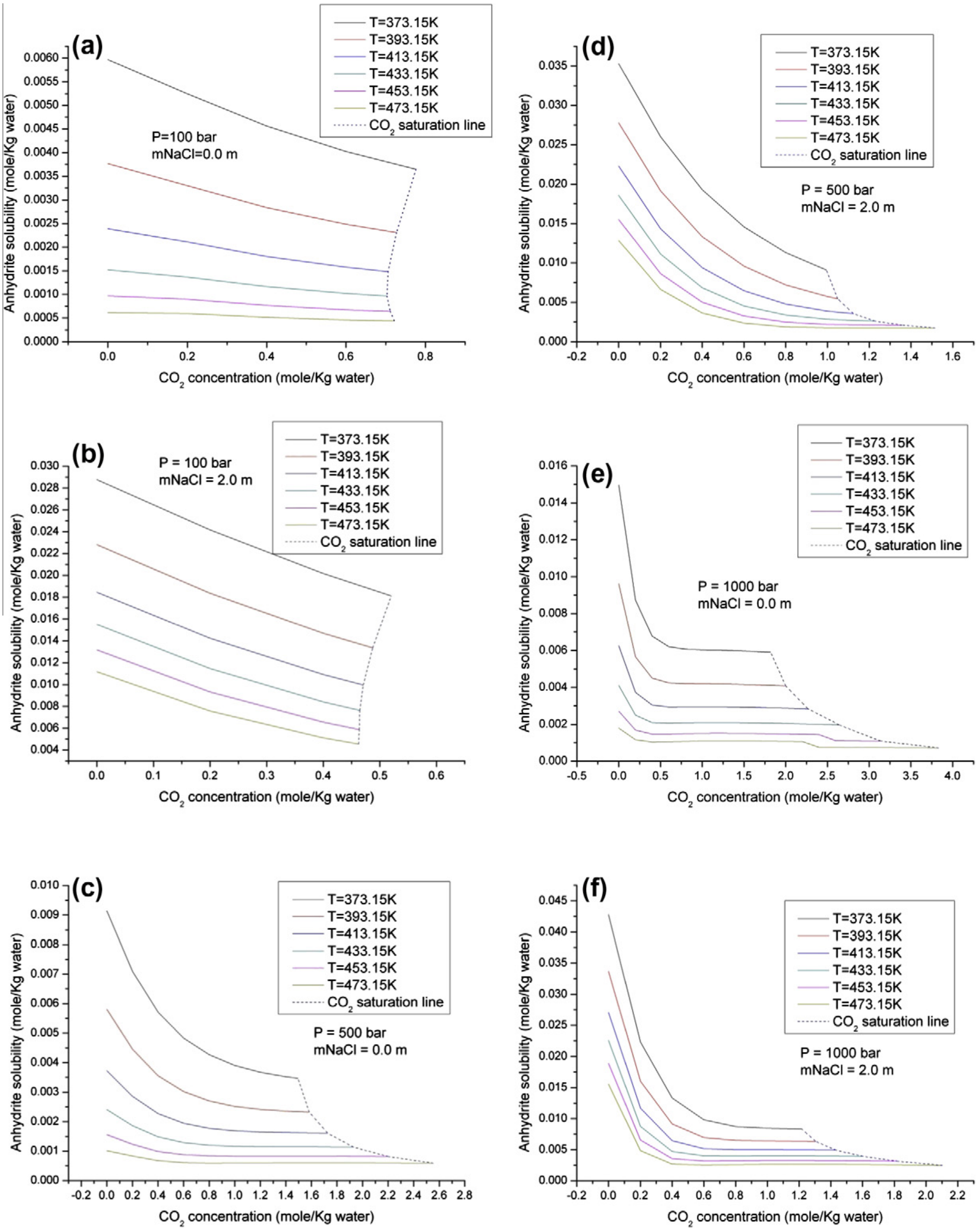

Fig. 14. Anhydrite solubility varying with CO_2 molality. (a) $P = 100$ bar, m_{NaCl} (NaCl molality) = 0; (b) $P = 100$ bar, $m_{NaCl} = 2.0$ m; (c) $P = 500$ bar, $m_{NaCl} = 0$; (d) $P = 500$ bar, $m_{NaCl} = 2.0$ m; (e) $P = 1000$ bar, $m_{NaCl} = 0$; (f) $P = 1000$ bar, $m_{NaCl} = 2.0$ m.

reliability of the model can be validated from the comparison of the model calculation with the experimental data as shown in Fig. 10. It can be concluded that the increase of NaCl molality may decrease the solubility of anhydrite at lower temperature and increase the solubility at higher temperature. For gypsum, we only have experimental data at 1 bar pressure. Compared with the limited experimental data, we can see that the model is generally within 10% of experimental data (Fig. 11). The addition of NaCl increases the solubility of gypsum up to about 3 m of NaCl, after that the solubility decreases slightly with the addition of NaCl. From Fig. 12a–c, the gypsum solubility variations with temperature are different for different NaCl molalities. From these figures, we can see the model accurately predicts the mineral solubility with remarkable predictability, considering the solubility data were not used in the parameterization.

So far, we have not found any experimental data on the gypsum or anhydrite solubility in CO_2 dissolved solutions. With the equilibrium model of CO_2–NaCl–$CaCO_3$–$CaSO_4$–H_2O system established, we can calculate the solubility of the two salts in the solution with CO_2 dissolved in it. Fig. 13 shows the gypsum solubility in CO_2 aqueous solution with CO_2 concentration from 0 to saturation. From the calculated results, we can see that gypsum solubility decreases with the increasing of CO_2 concentration at the different pressures. Fig. 14 shows the anhydrite solubility in CO_2 aqueous solution with CO_2 concentration from 0 to saturation. Like gypsum, the addition of CO_2 to the solution decreases the anhydrite solubility either in water or

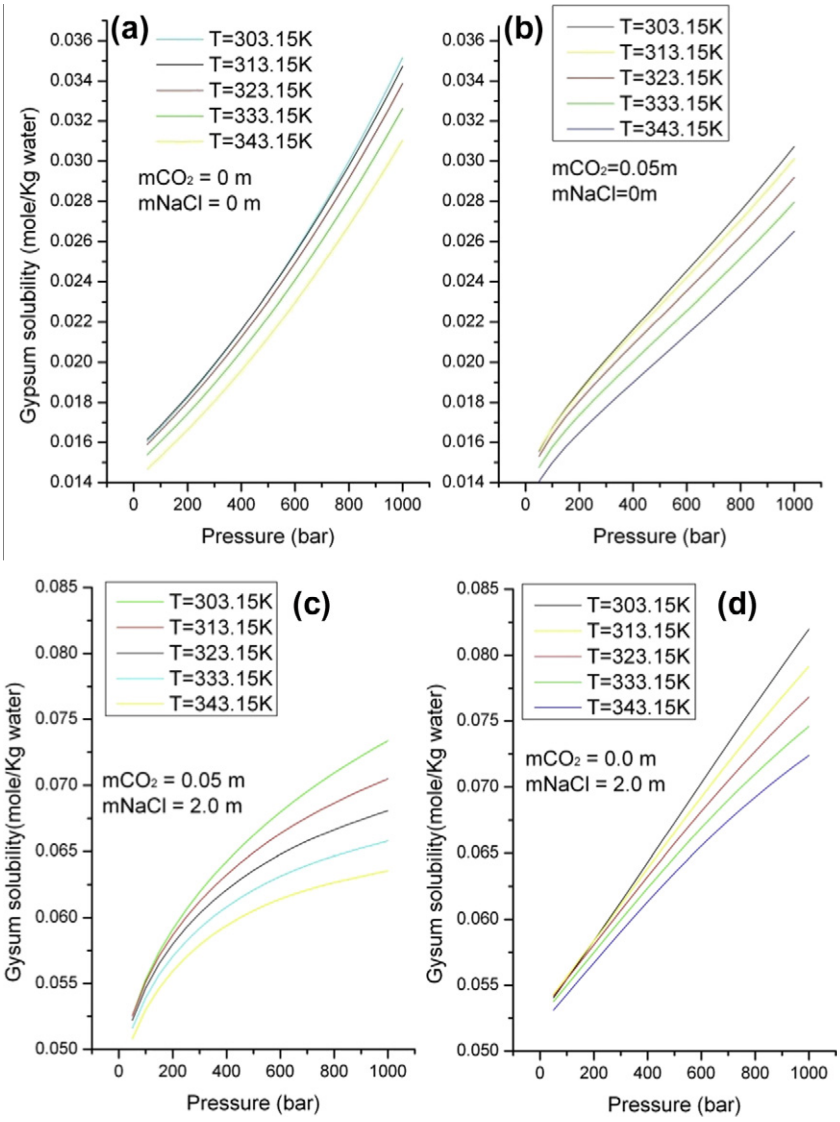

Fig. 15. Gypsum solubility varying with pressure in NaCl solution with CO_2 solved in it; (a) m_{NaCl} (the NaCl molality) = 0, m_{CO2} (the CO_2 molality) = 0; (b) $m_{NaCl} = 0$, $m_{CO2} = 0.05$ m; (c) $m_{NaCl} = 2.0$, $m_{CO2} = 0.05$ m; (d) $m_{NaCl} = 2.0$, $m_{CO2} = 0$.

NaCl solution. From Fig. 15, we can find that without CO_2 and NaCl in the solution, the gypsum solubility increases with pressure nearly linearly; when adding CO_2 and NaCl solved in the solution, the slop become smaller and even much smaller at higher pressures. The similar results can also be found for anhydrite. See Fig. 16.

3.1.2. Halite and calcite solubility

Halite and calcite solubility can be calculated from this model which can totally reproduce the results of its subsystem model (Duan and Li, 2008). When the component $CaSO_4$ are added in the solution, the solubilities of halite and calcite will change to some extent. Fig. 17 shows the comparison of halite solubility in water and in aqueous solution saturated with gypsum or anhydrite under different temperatures and pressures. In aqueous solution saturated with gypsum, halite solubility decreases by about 1% but halite solubility changes little if anhydrite is saturated because the anhydrite solubility in water is much lower than the solubility of halite in the $T-P$ range studied.

Fig. 18 shows the effect of the dissolution of anhydrite and gypsum on the calcite solubility. We can see that the calcite solubility in gypsum or anhydrite saturated solution is substantially reduced as compared with the solubility in

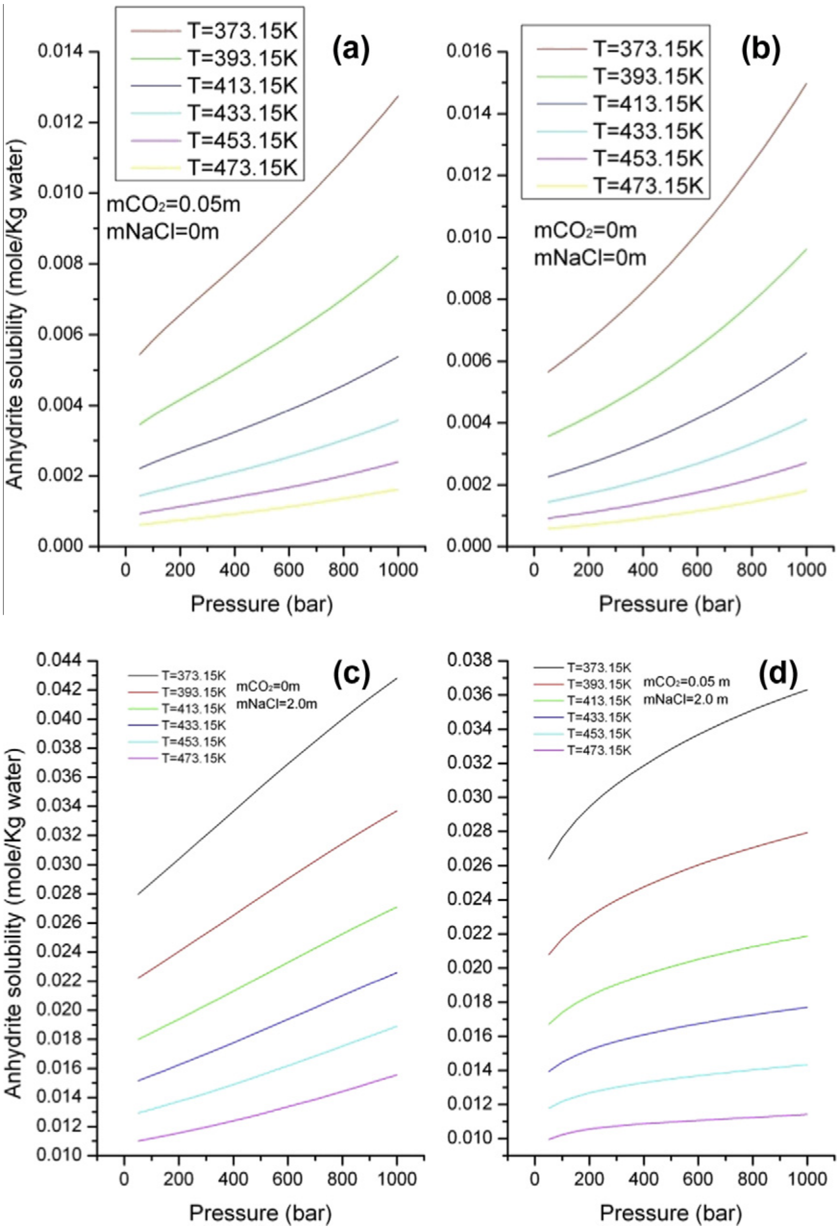

Fig. 16. Anhydrite solubility varying with pressure in NaCl solutions with CO_2 dissolved in it; (a) m_{NaCl} (the NaCl molality) = 0, m_{CO2} (the CO_2 molality) = 0.05 m; (b) $m_{NaCl} = 0$, $m_{CO2} = 0$; (c) $m_{NaCl} = 2.0$ m, $m_{CO2} = 0$; (d) $m_{NaCl} = 2.0$ m, $m_{CO2} = 0.05$ m.

pure water. Compared with calcite, the solubility of gypsum and anhydrite is large, so the molality of the cation Ca^{2+} is large. From Eqs. (17) and (10), we have $K_{10} = \frac{m_{\mathrm{Ca}^2+}\gamma_{\mathrm{Ca}^2+}m_{\mathrm{CO}_3^{2-}}\gamma_{\mathrm{CO}_3^{2-}}}{a_{\mathrm{CaCo}_3}}$ For $a_{\mathrm{CaCO}_3} = 1, K_{10} = m_{\mathrm{Ca}^{2+}}\gamma_{\mathrm{Ca}^{2+}}m_{\mathrm{CO}_3^{2-}}\gamma_{\mathrm{CO}_3^{2-}}$. At given temperature and pressure, is a constant, so when the molality of Ca^{2+} is large, the molality of CO_3^{2-} should be small. So the solubility of calcite become much smaller as gypsum or anhydrite solved in the solution. Conversely, the addition of calcite in water has little effect to the solubility of gypsum and anhydrite since the calcite solubility is small (Fig. 19).

3.2. Anhydrite – gypsum phase boundary in the TPX(temperature, pressure and NaCl molality) space

According to the phase rule, $f = C - P + 2$. Here, f is the degree of the freedom; C is the number of the components and P is the number of phases. When calcium sulfate is dissolved in NaCl aqueous solution, there are 3 components, and the number of phases P equals 3, liquid, anhydrite and gypsum. So, the degree of the freedom f is 2. That is to say, when pressure and the NaCl molality are given, the temperature of the three phase coexistence can be determined, vice versa. With our model, we can calculate the gypsum–anhydrite coexistent temperature, pressure and NaCl molality. In another word, when two of the above three variables are given, the other can be determined. For example, we set pressure and NaCl molality as variables, the coexistent temperature can be calculated, and we fit the result with an equation.

$$T = a_1 + a_2P + a_3P^2 + a_4m_{\mathrm{NaCl}} + a_5Pm_{\mathrm{NaCl}} + a_6P^2m_{\mathrm{NaCl}} + a_7m_{\mathrm{NaCl}}^2 + a_8m_{\mathrm{NaCl}}^2P \tag{28}$$

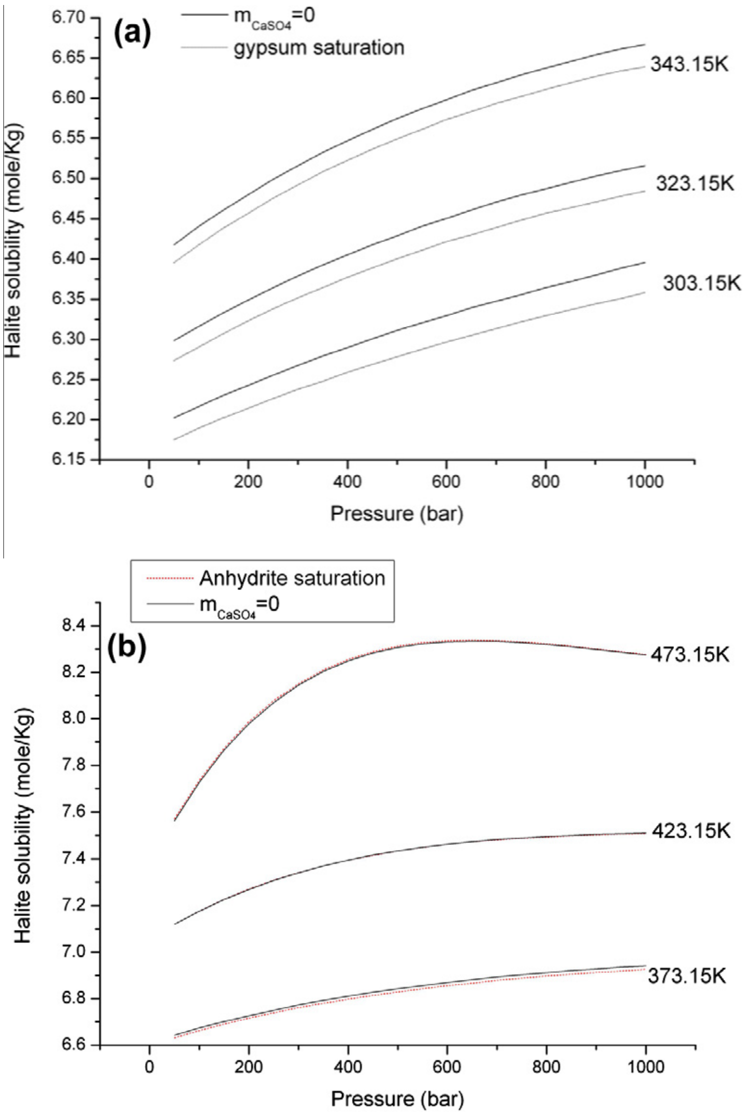

Fig. 17. Halite solubilities in pure water and in gypsum or anhydrite saturated solution varying with pressure at different temperatures.

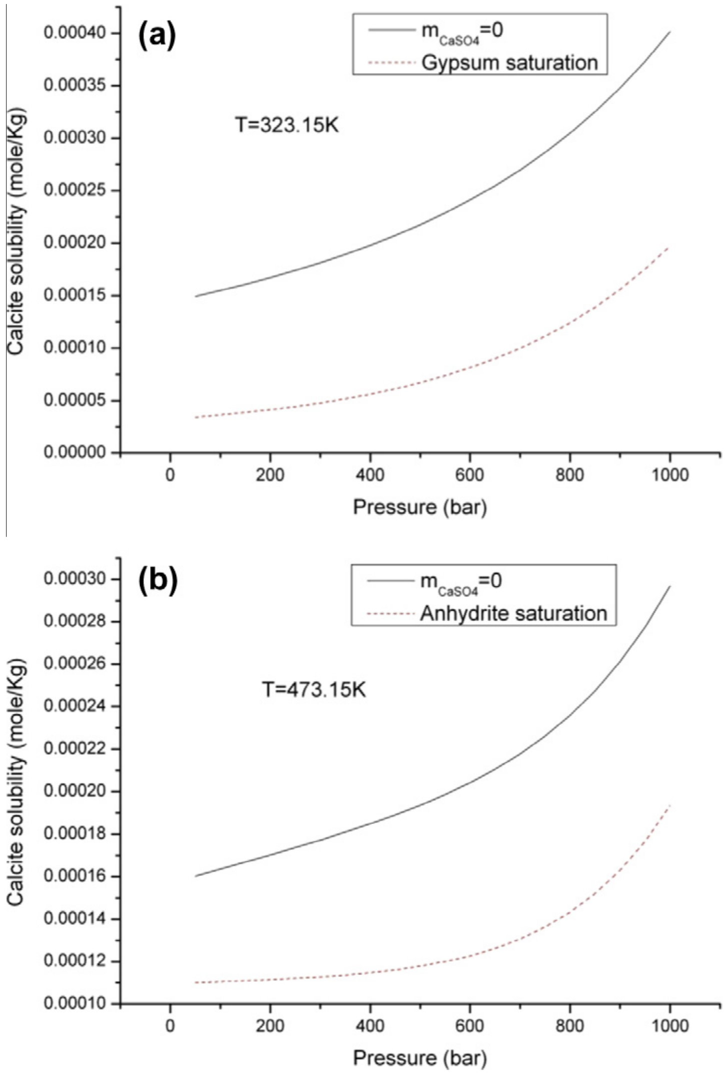

Fig. 18. Calcite solubilities in pure water and in gypsum or anhydrite saturated solution varying with pressure at different temperatures.

The parameters are listed in Table 7. Fig. 20 shows the coexistence temperature, pressure, and NaCl molality.

3.3. CO_2 solubility

Duan and Sun (2003) and Duan et al. (2006) established a model that can predict CO_2 solubility in NaCl solution with NaCl molality up to 4.5 mol/Kg accurately. The model of Duan and Li (2008) increased the upper limit of NaCl from 4.5 m to the saturation of halite with same high accuracy. With this model, CO_2 solubility can be predicted in the solutions with $CaSO_4$ salts, $CaCO_3$ salts and halite dissolved. As we know, $CaSO_4$ salts have very low solubility in water or NaCl solution, so their influence on CO_2 solubility is small which can be seen from Figs. 21 and 22.

3.4. pH value

pH value is a very important factor for predicting the dissolution and precipitation of the minerals in aqueous solutions. The pH value of the solution with CO_2–NaCl–$CaCO_3$–$CaSO_4$–H_2O can be calculated by the model. Figs. 23 and 24 show the variation of pH value in CO_2 saturated solution with pressure, temperature, NaCl molality and the concentration of anhydrite or gypsum. From the figures, we can find that the addition of anhydrite or gypsum will increase the pH value of the solution at lower pressures and decrease the pH value at higher pressures.

4. CONCLUSION

Based on our previous work on the H_2O–NaCl–CO_2–$CaCO_3$ system (Duan and Li), we developed a

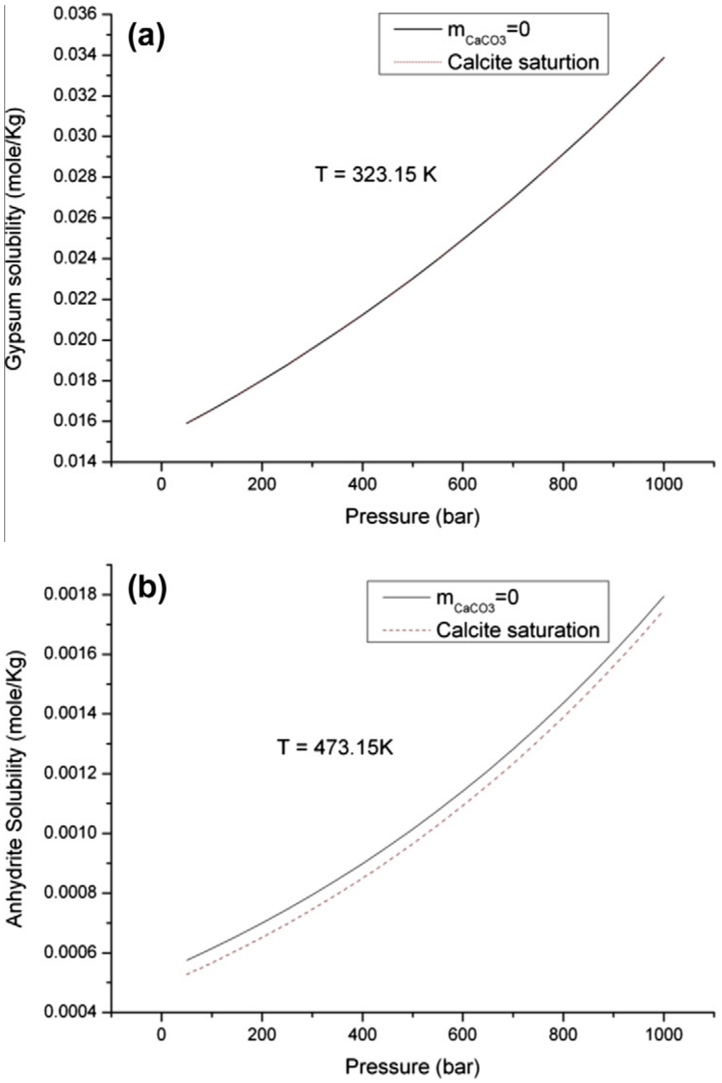

Fig. 19. Gypsum and anhydrite solubilities in pure water and calcite saturated solution varying with pressure at different temperatures.

thermodynamic equilibrium model for the quinary system, H_2O–CO_2–NaCl–$CaCO_3$–$CaSO_4$ from 25 to 250 °C and from 1 to 1000 bar up to high salinities. This model simultaneously calculates equilibrium of the vapor ($CO_2 + H_2O$), aqueous liquid phase (H^+, Na^+, Ca^{2+}, $CaHCO_3^+$, $Ca(OH)^+$, OH^-, Cl^-, HCO_3^-, HSO_4^-, SO_4^{2-}, CO_3^{2-}, $CO_{2(aq)}, CaCO_{3(aq)}$ and $CaSO_{4(aq)}$) and solid phases (halite, calcite, gypsum and anhydrite) as four solid phases.

Table 7
The parameters of coexistent temperature, pressure, and NaCl molality relation equation.

a_1	0.328158837806D+03
a_2	0.121400074586D−01
a_3	−.137086920950D−05
a_4	−.200540060072D+01
a_5	−.111430703466D−02
a_6	0.418805339550D−06
a_7	−.232129438458D+00
a_8	0.591930569232D−04

While increase one more component ($CaSO_4$) to the quaternary system substantially increases the complexity of modeling, all of the results of the previous model of Duan and Li (2008) can be reproduced by this model. The main contribution of this model can be summarized in three aspects: (1) The solubility of the minerals (calcite, halite gypsum and anhydrite) has been modeled as a function of temperature, pressure and salinity with accuracy close to experiment. In particular, the solubility of the minerals in aqueous solutions with NaCl, $CaCO_3$ and CO_2 can be predicted without fitting experimental data. The gypsum–anhydrite phase boundary can be predicted in the temperature-pressure space as a function of NaCl concentration; (2) the effect of dissolved $CaSO_4$ component in aqueous solutions on the solubilities of halite, calcite and CO_2 can be evaluated by this model. (3) The pH values,

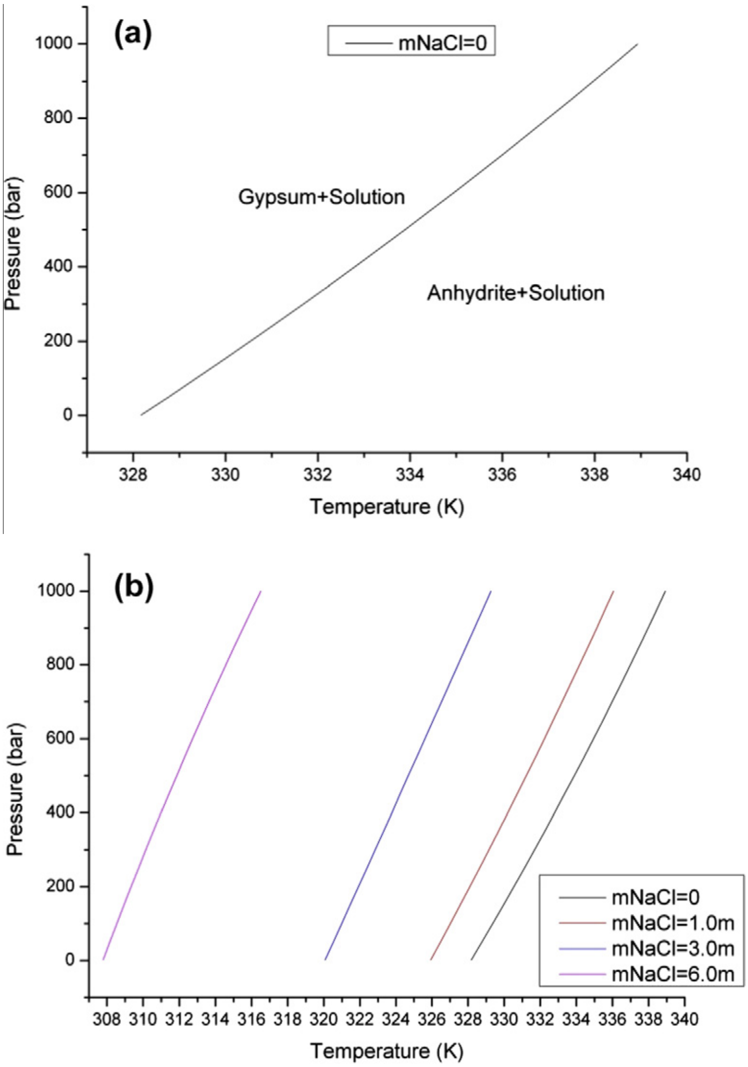

Fig. 20. Anhydrite and gypsum coexistent pressure and temperature at different NaCl molalities.

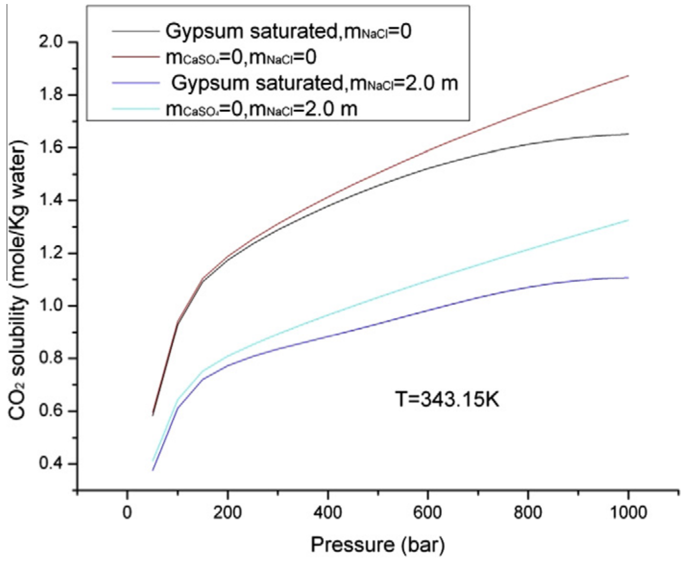

Fig. 21. Comparison of the CO_2 solubility in pure water and in aqueous solution saturated with gypsum at 343.15 K.

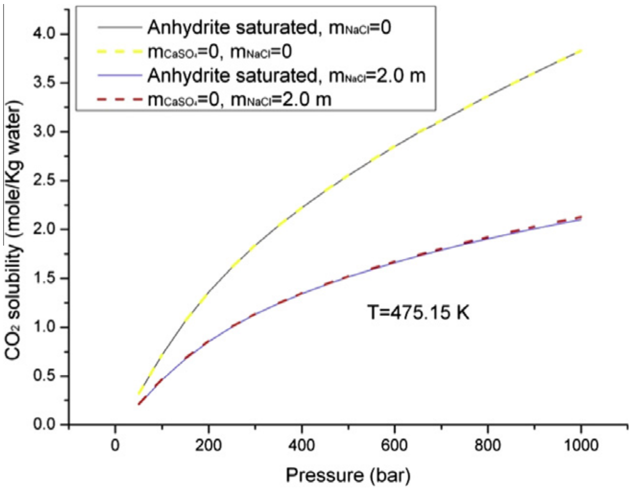

Fig. 22. Comparison of the CO_2 solubility in pure water and in aqueous solution with saturated with anhydrite at 475.15 K.

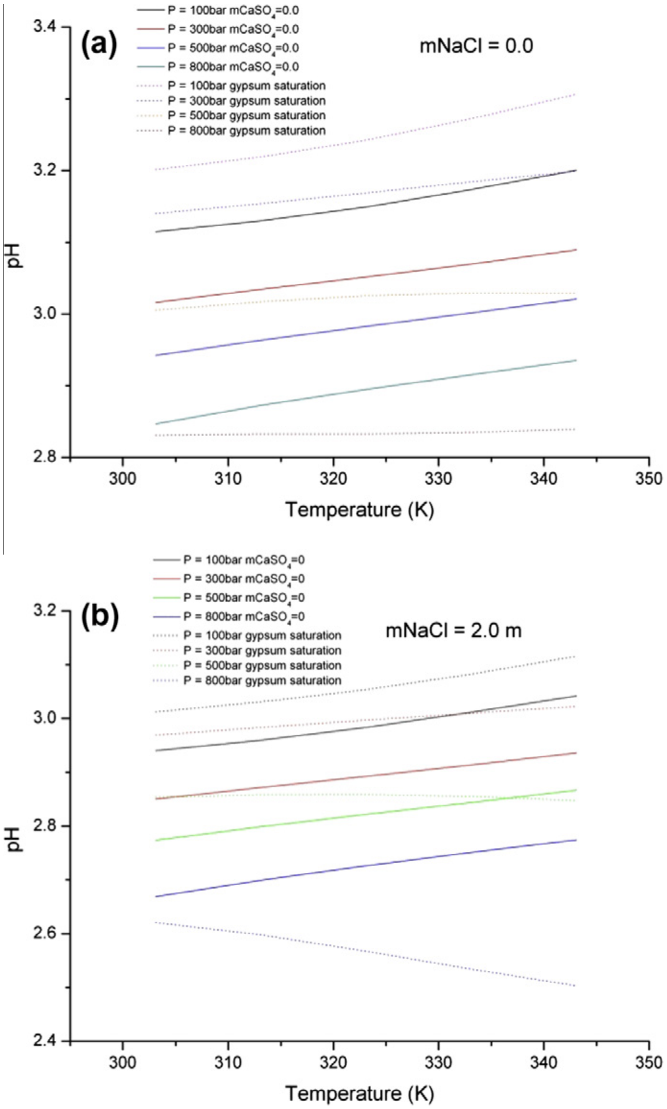

Fig. 23. pH values of aqueous solution with CO_2 and gypsum saturated in water; (a) m_{NaCl} (the NaCl molality) = 0; (b) m_{NaCl} = 2.0 m.

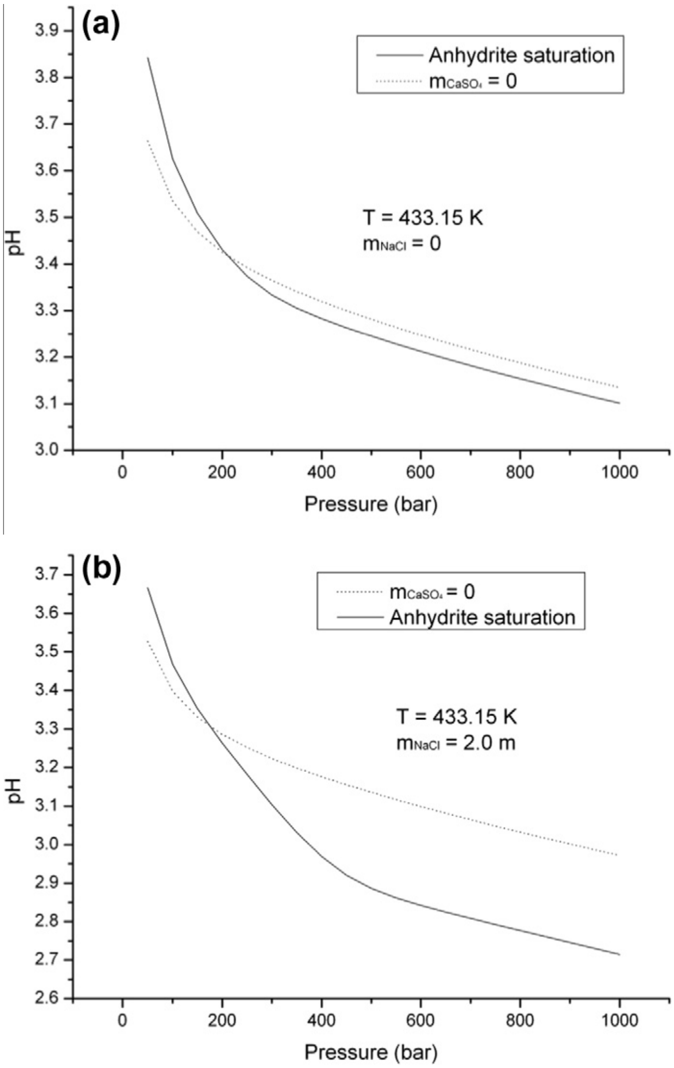

Fig. 24. pH values of solution with CO$_2$ and anhydrite saturated in water; (a) the NaCl molality $m_{\mathrm{NaCl}} = 0$; (b) the NaCl molality $m_{\mathrm{NaCl}} = 2.0$ m.

alkalinity and speciation reactions of aqueous solutions with CO$_2$, NaCl, CaCO$_3$ and CaSO$_4$ can be simultaneously calculated.

ACKNOWLEDGEMENTS

This research is supported by the National Science Foundation of China (Grants #90914010 and #41020134003 and #40873050). Thanks Drs. Li Dedong and Mao Shide for providing some source codes. Thanks also to Drs. Jean Dubbesy and Nikolay Akinfiev and an anonymous reviewer for their constructive comments and suggestions.

APPENDIX A. THE PITZER MODEL

The Pitzer model developed by Pitzer (1973) has the following form:

$$\begin{aligned}\sum\nolimits_i m_i(\phi - 1) = 2\Bigg(&-\frac{A^{\varphi} I^{\frac{3}{2}}}{1 + 1.2 I^{\frac{1}{2}}}\Bigg)\\ &+ \sum_{c=1}^{N_c}\sum_{a=1}^{N_a} m_c m_a \left(B_{ca}^{\phi} + Z C_{ca}\right)\\ &+ \sum_{c=1}^{N_c}\sum_{c=c+1}^{N_c} m_c m_c \left(\Phi_{cc'}^{\phi} + \sum_{a=1}^{N_a} m_a \psi_{cc'a}\right)\\ &+ \sum_{a=1}^{N_a}\sum_{a=a+1}^{N_a} m_a m_{a'} \left(\Phi_{aa'}^{\phi} + \sum_{c=1}^{N_c} m_c \psi_{aa'c}\right)\\ &+ \sum_{n=1}^{N_n}\sum_{a=1}^{N_a} m_n m_a \lambda_{na} + \sum_{n=1}^{N_n}\sum_{c=1}^{N_c} m_n m_c \lambda_{nc}\end{aligned} \tag{A1}$$

$$\begin{aligned}\ln\gamma_M &= z_M^2 F + \sum_{a=1}^{N_a} m_a(2B_{Ma} + ZC_{Ma}) \\ &\quad + \sum_{c=1}^{N_c} m_c\left(2\Phi_{Mc} + \sum_{a=1}^{N_a} m_a\psi_{Mca}\right) \\ &\quad + \sum_{a=1}^{N_a^{-1}} \sum_{a=a+1}^{N_a} m_a m_a \psi_{aa'M} + |z_M| \sum_{c=1}^{N_c}\sum_{a=1}^{N_a} m_c m_a C_{ca} \\ &\quad + \sum_{n=1}^{N_n} m_n(2\lambda_{nM}) + 6\sum_{n=1}^{N_n}\sum_{a=1}^{N_a} m_n m_a \zeta_{\mathrm{Mna}} \qquad \text{(A2)}\end{aligned}$$

$$\begin{aligned}\ln\gamma_X &= z_X^2 F + \sum_{c=1}^{N_c} m_c(2B_{cX} + ZC_{cX}) \\ &\quad + \sum_{a=1}^{N_a} m_a\left(2\Phi_{Xa} + \sum_{c=1}^{N_c} m_c\psi_{Xac}\right) \\ &\quad + \sum_{c=1}^{N_c^{-1}} \sum_{c'=c+1}^{N_c} m_c m_{c'} \psi_{cc'X} + |z_M| \\ &\quad + \sum_{c=1}^{N_c}\sum_{a=1}^{N_a} m_c m_a C_{ca} + \sum_{n=1}^{N_n} m_n(2\lambda_{nX}) \\ &\quad + 6\sum_{n=1}^{N_n}\sum_{c=1}^{N_c} m_n m_c \zeta_{ncX} \qquad \text{(A3)}\end{aligned}$$

$$\begin{aligned}\ln\gamma_N &= 2\sum_{n=1}^{N_n} m_n\lambda_{Nn} + 2\sum_{c=1}^{N_c} m_c\lambda_{Nc} + 2\sum_{a=1}^{N_a} m_a\lambda_{Na} \\ &\quad + \sum_{c=1}^{N_c}\sum_{a=1}^{N_a} m_c m_a \lambda_{Nca} \qquad \text{(A4)}\end{aligned}$$

where ϕ is the osmotic coefficient of the solvent. Φ is the second virial coefficient. λ and ζ are second-order and third-order interaction parameters, respectively. m_c and z_c are the molality and the charge of cation c. N_c is the total number of cations. Similar definitions apply for anions, a, and neutrals, n. The subscripts M, X and N refer to cations, anions, and neutrals, respectively. F is defined by

$$\begin{aligned}F &= -A^{\phi}\left(\frac{1^{1/2}}{1+1.2I^{1/2}} + \frac{2}{1.2}\ln(1+1.2I^{1/2})\right) \\ &\quad + \sum_{c=1}^{Nc}\sum_{a=1}^{Na} m_c m_{c'} m'_{cc'} B'_{ca} + \sum_{c=1}^{N_c-1}\sum_{c=c+1}^{N_c} m_c m'_c \Phi'_{cc'} \\ &\quad + \sum_{a=1}^{N_a-1}\sum_{a=a+1}^{Na} m_a m_{a'} \Phi'_{aa'} \qquad \text{(A5)}\end{aligned}$$

$$C_{MX} = C_{MX}^{\phi}/2|Z_M Z_X|^2 \qquad \text{(A6)}$$

$$Z = \sum_i |z_i| m_i \qquad \text{(A7)}$$

$$B_{MX}^{\phi} = \beta_{MX}^{(0)} + \beta_{MX}^{(1)} e - \alpha MX\sqrt{I} + \beta_{MX}^{(2)} e - 12\sqrt{I} \qquad \text{(A8)}$$

$$B_{MX} = \beta_{MX}^{(0)} + \beta_{MX}^{(1)} g(\alpha_{MX}\sqrt{I}) + \beta_{MX}^{(2)} g(12\sqrt{I}) \qquad \text{(A9)}$$

$$B'_{MX} = \beta_{MX}^{(1)} g'(\alpha_{MX}\sqrt{I})/I + \beta_{MX}^{(2)} g'(12\sqrt{I})/I \qquad \text{(A10)}$$

$$g(x) = 2(1-(1+x)e^{-x})/X^2 \qquad \text{(A11)}$$

$$\Phi_{ij}^{\phi} = \theta_{ij} + {}^{E}\theta_{ij}(I) + I^{E}\theta'_{ij}(I) \qquad \text{(A12)}$$

$$\Phi_{ij} = \theta_{ij} + {}^{E}\theta_{ij}(I) \qquad \text{(A13)}$$

$$\Phi'_{ij} = {}^{E}\theta'_{ij}(I) \qquad \text{(A14)}$$

$${}^{E}\theta_{MN}(I) = \frac{z_M z_N}{4I}\left(J_0(X_{MN}) - \frac{1}{2}J_0(X_{MM}) - \frac{1}{2}J_0(X_{NN})\right) \qquad \text{(A15)}$$

$${}^{E}\theta'_{MN}(I) = \frac{z_M {z_N}^2}{8I}\left(J_1(X_{MN}) - \frac{1}{2}J_1(X_{MM}) - \frac{1}{2}J_1(X_{NN})\right) - \frac{{}^{E}\theta_{MN}(I)}{I} \qquad \text{(A16)}$$

where $X_{MN} = 6z_M z_N A^{\phi}\sqrt{\mathrm{I}}$.

$$J_0(X) = \frac{1}{4}x - 1 + \frac{1}{x}\int_0^{\infty}\left[1 - \exp\left(-\frac{x}{y}\right)e^{-y}\right]y^2 dy$$

$$J_1(X) = \frac{1}{4}x - \frac{1}{x}\int_0^{\infty}\left[1 - \left(1 + \frac{x}{y}e^{-y}\right) \times \exp\left(-\frac{x}{y}e^{-y}\right)\right]y^2 dy$$

where A^{ϕ} is one third the Debye–Huckel limiting slope. What we need to do is to determine the Pitzer parameters, $\beta_{MX}^{(0)}, \beta_{MX}^{(1)}, \beta_{MX}^{(2)}$ and C_{MX}^{φ} for each cation–anion pair, θ_{ij} for each cation–cation or anion–anion pair; Ψ_{ijk} for each cation–cation–anion and anion–anion–cation triplet, λ_{ni} for ion–neural pairs, and ζ_{nij} for neutral–anion–cation triplet.

REFERENCES

Anderson G. M., Crerar S., Schott J. and Mesmer R. E. (1991) The density model for estimation of thermodynamic parameters of reactions at high-temperatures and pressures. *Geochim. Cosmochim. Acta* **55**(7), 1769–1779.

Arslan A. and Dutt G. R. (1993) Solubility of gypsum and its prediction in aqueous solutions of mixed electrolytes. *Soil Sci.* **155**(1), 37–47.

Azimi G., Papangelakis V. G. and Dutrizac J. E. (2007) Modelling of calcium sulphate solubility in concentrated multi-component sulphate solutions. *Fluid Phase Equilibria* **260**, 300–315.

Bermejo M. D., Martin A., Florusse L. J., Peters C. J. and Cocero M. J. (2005) The influence of Na_2SO_4 on the CO_2 solubility in water at high pressure. *Fluid Phase Equilibrium* **238**, 220–228.

Blount C. W. and Dickson F. W. (1969) The solubility of anhydrite ($CaSO_4$) in NaCl–H_2O from 100 to 450° and 1–1000 bars. *Geochim. Cosmochim. Acta* **33**, 227–245.

Blount C. W. and Dickson F. W. (1973) Gypsum–Anhydrite equilibrium in systems $CaSO_4$–H_2O and $CaSO_4$–NaCl–H_2O. *Am. Mineralog.* **58**, 323–331.

Bock E. (1961) On the solubility of anhydrous calcium sulfate and gypsum in concentrated solutions of sodium chloride at 25 °C, 30 °C, 40 °C, and 50 °C. *Can. J. Chem.* **39**, 1746–1751.

Booth H. S. and Bidwell R. M. (1950) Solubilities of salts in water at high temperatures. *J. Am. Chem. Soc.* **72**, 2567–2575.

Busey R. H. and Mesmer R. E. (1978) Thermodynamic quantities for the ionization of water in sodium chloride media to 300 °C. *J. Chem. Eng. Data* **23**, 175–176.

Christov C. and Møller N. (2004a) Chemical equilibrium model of solution behavior and solubility in H–Na–K–OH–Cl–HSO_4–SO_4–H_2O system to high concentration and temperature. *Geochim. Cosmochim. Acta* **68**(6), 1309–1331.

Christov C. and Møller N. (2004b) A chemical equilibrium model of solution behavior and solubility in the H–Na–K–Ca–OH–Cl–HSO_4–SO_4–H_2O system to high concentration and temperature. *Geochim. Cosmochim. Acta* **68**(18), 3717–3719.

D'Ans J., Bredtschneider D., Eick H. and Freund H. E. (1955) Untersuchungen uber die calcium sulfate. *Kali. U. Steinsalz* **5**, 109–111.

Denman W. L. (1961) Maximum re-use of cooling water based on gypsum content and solubility. *Ind. Eng. Chem.* **53**, 817–822.

Dickson F. W., Blount C. W. and Tuell G. (1963) Use of hydrothermal solution equipment to determine the solubility of anhydrite in water from 100 °C to 275 °C and from 1 bar to 1000 bar pressure. *Am. J. Sci.* **261**, 61–78.

Duan Z. and Li D. (2008) Coupled phase and aqueous species equilibrium of the H_2O–CO_2–NaCl–$CaCO_3$ system from 0 to 250 °C, 1–1000 bar with NaCl concentrations up to saturation of halite. *Geochim. Cosmochim. Acta*, 72.

Duan Z., Moller N. and Weare J. (1995) Measurements of the PVT properties of water to 25 kbars and 1600 °C from synthetic fluid inclusions in Corundum. *Geochim. Cosmochim. Acta* **59**, 2693.

Duan Z. and Sun R. (2003) An improved model calculating CO_2 solubility in pure water and aqueous NaCl solutions from 273 to 533 K and from 0 to 2000 bar. *Chem. Geol.* **193**(3–4), 253–271.

Duan Z., Sun R., Zhu C. and Chou I.-M. (2006) An improved model for the calculation of CO_2 solubility in aqueous solutions containing Na^+, K^+, Ca^{2+}, Mg^{2+}, Cl^-, and SO_4^{2-}. *Marine Chem.* **98**(2–4), 131–139.

Giles M. R. (1987) Mass transfer and problems of secondary porosity creation in deeply buried hydrocarbon reservoirs. *Mar. Petrol. Geol.* **4**(3), 188–204.

Greenberg J. P. and Møller N. (1989) The prediction of mineral solubilities in natural waters: a chemical equilibrium model for the Na–K–Ca–Cl–SO_4–H_2O system to high concentration from 0 to 250 °C. *Geochim. Cosmochim. Acta* **53**, 2503–2518.

Hall R. E., Robb J. A. and Coleman C. E. (1926) The solubility of calcium sulfate at boiler-water temperatures. *J. Am. Chem. Soc.* **48**, 3733–3738.

Hardie L. A. (1967) The gypsum–anhydrite equilibrium at 1 atmosphere pressure. *Am. Mineral.* **52**, 171–200.

Harvie C. E., Møller N. and Weare J. H. (1984) The prediction of mineral solubilities in natural waters: the Na–K–Mg–Ca–H–Cl–SO_4–OH–HCO_3–CO_3–CO_2–H_2O system to high ionic strengths at 25 °C. *Geochim. Cosmochim. Acta* **48**(4), 723–751.

Harvie C. E. and Weare J. H. (1980) The prediction of mineral solubilities in natural waters: the Na–K–Mg–Ca-Cl-SO_4–H_2O system from zero to high concentration at 25 °C. *Geochim. Cosmochim. Acta* **44**(7), 981–997.

Helgeson H. C. (1969) Thermodynamics of hydrothermal systems at elevated temperatures and pressures. *Am. J. Sci.* **267**(7), 729–804.

Helgeson H. C., Delany J. M., Nesbitt H. W. and Bird D. K. (1978) Summary and critique of the thermodynamic properties of rock-forming minerals. *Am. J. Sci.*, 278-A.

Helgeson H. C. and Kirkham D. H. (1976) Theoretical prediction of the thermodynamic behavior of aqueous electrolytes at high pressures and temperatures: III. Equation of state for aqueous species at infinite dilution. *Am. J. Sci.* **276**, 97–240.

Helgeson H. C., Kirkham D. H. and Flowers G. C. (1981) Theoretical prediction of the thermodynamic behavior of aqueous electrolytes at high pressures and temperatures: calculation of activity coefficients, osmotic coefficients, and apparent molal and standard and relative partial modal properties to 600 °C and 5 Kb. *Am. J. Sci.* **281**, 1249–1516.

Hill A. E. (1937) The transition temperature of gypsum to anhydrite. *Contribution From The Chemical Laboratories of New York University* **59**, 2242–2244.

Hulett and Allen L. E. (1902) The solubility of gypsum. *J. Am. Chem. Soc.* **24**, 667–679.

Johnson J. W., Oelkers E. H. and Helgeson H. C. (1992) SUPCRT92: a software package for calculating the standard molal thermodynamic properties of minerals, gases, aqueous species, and reactions from 1 to 5000 bar and 0–1000 °C. *Comput. Geosci.* **18**(7), 899–947.

Li D. and Duan Z. (2007) The speciation equilibrium coupling with phase equilibrium in the H_2O–CO_2–NaCl system from 0 to 250 °C, from 0 to 1000 bar, and from 0 to 5 molality of NaCl. *Chem. Geol.* **244**, 730–751.

Li L., Peters C. A. and Celia M. A. (2007) Effects of mineral spatial distribution on reaction rates in porous media. *Water Resources Res.* **43**(1).

Møller N. (1988) The prediction of mineral solubilities in natural waters: a chemical equilibrium model for the Na–Ca–Cl–SO_4–H_2O system, to high temperature and concentration. *Geochim. Cosmochim. Acta* **52**, 821–837.

Madgin W. M. and Swales D. A. (1956) Solubilities in the system $CaSO_4$–NaCl–H_2O at 25° and 35°. *J. Appl. Chem.* **6**, 482–487.

Marshall W. J. and Slusher R. (1966) Thermodynamics of calcium sulfate dihydrate in aqueous sodium chloride solutions, 0–110°. *J. Phys. Chem.* **70**, 4015–4027.

Marshall W. J., Slusher R. and Jones E. V. (1964) Aqueous systems at high temperature XIV. Solubility and thermodynamic relationships for $CaSO_4$ in NaCl–H_2O solutions from 40 °C to 200 °C, 0–4 Molal NaCl. *J. Chem. Eng. Data* **9**, 187–191.

Melcher A. C. (1910) The solubility of silver chloride barium sulfate and calcium sulfate at high temperatures. *J. Am. Chem. Soc.* **32**, 50–66.

Mesmer R. E., Marshall W. L., Palmer D. A., Simonson J. M. and Holmes H. F. (1988) Thermodynamics of aqueous association and ionization reactions at high-temperature and pressures. *J. Solut. Chem.* **17**(8), 699–718.

Millero F. J. (1982) The effect of pressure on the solubility of minerals in water and seawater. *Geochim. Cosmochim. Acta* **46**, 11–22.

Morey G. W. and Hesselgesser J. M. (1951) The solubilities of some minerals in super-heated steam at high pressure. *Econ. Geol.* **46**, 821–835.

Partridge E. P. and White A. H. (1929) The solubility of calcium sulfate from 0 to 200 °C. *J. Am. Chem. Soc.* **51**, 360–370.

Pitzer K. S. (1973) Thermodynamics of electrolytes I. Theoretical basis and general equations. *J. Phys. Chem.* **77**(2), 268–277.

Pitzer K. S. and Kim J. J. (1974) Thermodynamics of electrolytes. IV. Activity and osmotic coefficients for strong electrolytes with one or both ions univalent. *J. Am. Chem. Soc.* **96**(18), 5701–5707.

Pitzer K. S. and Mayorga G. (1973) Thermodynamics of electrolytes. II. Activity and osmotic coefficients for strong electrolytes with one or both ions univalent. *J. Phys. Chem.* **77**(19), 2300–2308.

Posnjak E. (1938) The system, $CaSO_4$–H_2O. *Am. J. Sci.*, 247–272.

Power W. H. and Fabuss B. M. (1964) Thermodynamic properties of saline water. In *Research and Development Process Report No. 104*, Office of Saline Water, US Department of the Interior, p. 82.

Power W. H., Fabuss B. M. and Scattebtdsld C. N. (1966) Transient solute concentrations and phase changes of calcium sulfate in aqueous sodium chloride. *J. Chem. Eng. Data* **11**, 149–154.

Pruess K. and Spycher N. (2007) ECO2N-a fluid property module for the TOUGH2 code for studies of CO_2 storage in saline aquifers. *Energy Convers. Manage.* **48**(6).

Ruaya J. R. (1988) Estimation of instability constants of metal chloride complexes in hydrothermal solutions up to 300 °C. *Geochim. Cosmochim. Acta* **52**(8), 218–229.

Rumpf B. and Maurer G. (1993) An experimental and theoretical investigation on the solubility of carbon dioxide in aqueous solutions of strong electrolytes. *Ber. Bunsenges. Phys. Chem.* **97**(1), 85–97.

Shock E. L. and Helgeson H. C. (1988) Calculation of the thermodynamic and transport properties of aqueous species at high pressures and temperature: correlation algorithms for ionic species and equation of state predictions to 5 Kb and 1000 °C. *Geochim. Cosmochim. Acta* **52**, 2009–2036.

Shock E. L., Oelkers E. H., Johnson J. W., Sverjensky D. A. and Helgeson H. C. (1992) Calculation of the thermodynamic properties of aqueous species at high pressures and temperatures. Effective electrostatic radii, dissociation constants and standard partial molal properties to 1000 °C and 5 kbar. *J. Chem. Soc. Faraday Trans.* **88**, 803–826.

Straub F. G. (1932) Solubility of calcium sulfate and calcium carbonate at temperatures between 182 °C and 316 °C. *Ind. Eng. Chem.* **24**, 914–917.

Styrikovich M. A. and Khokhlov L. K. (1957) Investigation of the solubility of salts in steam at supercritical parameters. *Teploenergy* **4**, 3–7.

Sverjensky D. A., Shock E. L. and Helgeson H. C. (1997) Prediction of the thermodynamic properties of aqueous metal complexes to 1000 °C and 5 Kb. *Geochim. Cosmochim. Acta* **61**(7), 1359–1412.

Tanger J. C. and Helgeson H. C. (1988) Calculation of the thermodynamic and transport-properties of aqueous species at high-pressures and temperatures: revised equations of state for the standard partial molal properties of ions and electrolytes. *Am. J. Sci.* **288**(1), 19–98.

Zanbak C. and Arthur R. C. (1986) Geochemical and engineering aspects of anhydrite/gypsum phase transitions. *Bull. Assoc. Eng. Geol.* **27**(4), 419–433.

Zen E.-A. (1965) Solubility measurements in the system $CaSO_4$–NaCl–H_2O at 35°, 50°, and 70 °C and one atmosphere pressure. *J. Petrol.* **6**, 124–164.

Associate editor: Chen Zhu